
Co-Representation Neural Hypergraph Diffusion for Edge-Dependent Node Classification

Yijia Zheng Marcel Worring
University of Amsterdam, Amsterdam, the Netherlands
{y.zheng, m.worring}@uva.nl

Abstract

Hypergraphs are widely employed to represent complex higher-order relationships in real-world applications. Most hypergraph learning research focuses on node- or edge-level tasks. A practically relevant but more challenging task, edge-dependent node classification (ENC), is only recently proposed. In ENC, a node can have different labels across different hyperedges, which requires the modeling of node-hyperedge pairs instead of single nodes or hyperedges. Existing solutions for this task are based on message passing and model within-edge and within-node interactions as multi-input single-output functions. This brings **three limitations**: (1) non-adaptive representation size, (2) node/edge agnostic messages, and (3) insufficient interactions among nodes or hyperedges. To tackle these limitations, we develop **CoNHD**, a new solution based on hypergraph diffusion. Specifically, we first extend hypergraph diffusion using node-hyperedge co-representations. This extension explicitly models both within-edge and within-node interactions as multi-input multi-output functions using two equivariant diffusion operators. To avoid handcrafted regularization functions, we propose a neural implementation for the co-representation hypergraph diffusion process. Extensive experiments demonstrate the effectiveness and efficiency of the proposed CoNHD model.

1 Introduction

Real-world applications often involve intricate higher-order relationships that cannot be represented by traditional graphs with pairwise connections [1–4]. Hypergraphs, where an edge can connect more than two nodes, provide a flexible structure to represent these relationships [5–8]. Many hypergraph learning methods are proposed to learn effective node or hyperedge representations [9–11]. These methods, however, are insufficient for predicting labels related to node-hyperedge pairs. For example, in a co-authorship hypergraph, a researcher may contribute differently to various academic papers, taking on distinct roles such as the first or last author. To initiate the development of effective solutions for such scenarios, Choe et al. [12] propose a new problem namely *edge-dependent node classification* (ENC), where a node can have different labels across different hyperedges. Addressing this problem requires modeling the node features unique to each hyperedge, which is more complex and requires considering the hypergraph structure. Despite its importance and usefulness in many real-world applications [13–16], the ENC problem is still under-explored.

Previous work on ENC only explores solutions using message passing-based hypergraph neural networks (HGNNs) [17, 18]. To avoid confusion, in this paper, *message passing* refers specifically to the HGNN architecture illustrated in Fig. 1(b), which employs a two-stage aggregation process. The first stage aggregates messages from nodes to update the hyperedge representation, while the second stage aggregates messages from hyperedges to update the node representation. The edge and node

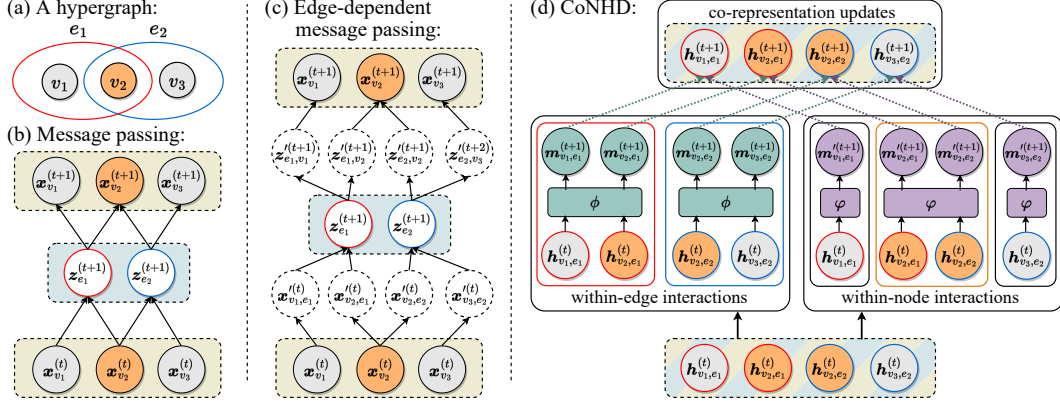


Figure 1: **Different HGNN architectures.** (a) A hypergraph example with three nodes and two hyperedges. (b) The message passing framework aggregates messages from nodes to hyperedges and then from hyperedges back to nodes. (c) Edge-dependent message passing methods extract edge(node)-dependent node(edge) representations (dashed circle) before aggregation. (d) CoNHD learns a co-representation, instead of separate node and hyperedge representations, for each node-hyperedge pair. Two equivariant neural diffusion operators, *i.e.*, ϕ and φ , model the within-edge and within-node interactions as multi-input multi-output functions, which can generate different diffusing information for different node-hyperedge pairs. The within-edge and within-node diffusing information is then utilized to update the co-representations.

representations are then concatenated and used to predict edge-dependent node labels [12]. Message passing is simple and intuitive, but does it yield the most effective solution?

To study the characteristics of message passing, we analyze its input-output relations. The two-stage aggregation process in message passing essentially models two key types of interactions: *within-edge interactions* (different nodes connected by a hyperedge) and *within-node interactions* (different hyperedges sharing a common node). Message passing models these interactions as *multi-input single-output* aggregation functions, which brings **three limitations**:

- **Non-adaptive representation size.** Considering within-node interactions, messages from numerous hyperedges are aggregated to a fixed-size node representation vector. As indicated in [19], this can cause potential information loss for large-degree nodes, which have more neighboring hyperedges and should have larger representation size. Analogously, the edge representations suffer from the same problem.
- **Node/Edge agnostic messages.** As the aggregated node representation loses edge-dependent information, the node can only pass the same message to different hyperedges. However, different hyperedges may focus on different properties of the node and should receive different messages. While some methods, as shown in Fig. 1(c), attempt to extract edge-dependent information from one node representation [19, 20, 12], this extraction process increases the learning difficulty.
- **Insufficient interactions among nodes or hyperedges.** The single-output design cannot include direct nodes-to-nodes or edges-to-edges interactions, as this requires multiple outputs for different elements. These direct interactions are shown to be critical for hypergraph learning [21].

To tackle the limitations of message passing and to develop an effective ENC solution, we should model the within-edge and within-node interactions as *multi-input multi-output* functions.

We develop a new solution based on hypergraph diffusion [22–25]. (Hyper)graph diffusion is inspired by physical diffusion processes, where information on each node propagates to its neighboring nodes through diffusion operators [26, 27]. As indicated in [20], an important characteristic of hypergraph diffusion operators is the permutation equivariance property, which means that reordering the inputs of the operator leads to corresponding outputs in the same order. As the hyperedges and nodes are inherently unordered, equivariance is necessary for modeling the *multi-input multi-output* interactions, which ensures that the output for each element is unaffected by the input ordering. Previous hypergraph diffusion models, however, only consider nodes-to-nodes interactions without representations for the hyperedges, which is not sufficient for ENC. In this paper, we extend the concept of hypergraph diffusion to make it applicable to the ENC problem.

We propose **CoNHD** (**Co**-representation **N**eural **H**ypergraph **D**iffusion), an effective hypergraph neural network based on hypergraph diffusion. We first extend hypergraph diffusion to learn node-hyperedge co-representations, enabling its application for ENC. This extension can model both within-edge and within-node interactions as multi-input multi-output functions. Furthermore, we present a neural implementation for co-representation hypergraph diffusion, which can adaptively learn suitable diffusion operators from the data. The general framework is shown in Fig. 1(d).

Our main contributions are summarized as follow:

1. We define **co-representation hypergraph diffusion**, a new concept that generalizes hypergraph diffusion using node-hyperedge co-representations. This allows the extension of existing hypergraph diffusion methods to tackle the ENC problem.
2. We propose **CoNHD**, a neural implementation for the co-representation hypergraph diffusion process. This naturally leads to a novel and effective HGNN architecture that can easily adapt to different ENC datasets.
3. We conduct extensive experiments to validate the **effectiveness** and **efficiency** of CoNHD. The results demonstrate that CoNHD can achieve the best performance on six real-world ENC datasets without sacrificing efficiency.

2 Related Work

Hypergraph Neural Networks. Inspired by the success of graph neural networks (GNNs) [28–30], hypergraph neural networks (HGNNs) have been proposed for modeling complex higher-order relationships [31–33]. HyperGNN [34, 35] and HCHA [36] define hypergraph convolution based on the clique expansion graph. HyperGCN [37] reduces the clique expansion graph into an incomplete graph with mediators. To directly utilize higher-order structures, HNHN [38] and HyperSAGE [17] model the convolution layer as a two-stage message passing process, where messages are first aggregated from nodes to hyperedges and then back to nodes. HyperGAT [39] incorporates an attention mechanism during aggregation. UniGNN [18] and AllSet [40] show that most existing HGNNs can be represented in this two-stage message passing framework. Recent research investigates edge-dependent node information in the aggregation process of message passing [19, 20, 12, 41].

While most HGNN research focuses on node- or hyperedge-level tasks, like node classification [42–44], node regression [45, 46], and edge reconstruction [47, 48], the ENC problem remains less explored. The first to explore the ENC problem is [12], which proposes WHATsNet, a solution based on message passing. Although message passing has become the dominant framework in existing HGNN research, it suffers from the limitations as discussed in the introduction due to the multi-input single-output design and cannot effectively address the ENC problem.

Hypergraph Diffusion. (Hyper)graph diffusion, taking inspiration from physical diffusion processes, describes the process of information propagating from each node to its neighboring nodes [49, 27]. The diffusing information is modeled as the gradients derived from the edge regularization functions, which provide regularization to the node representations within the same hyperedge [24]. These functions are handcrafted without training weights. The technique was first introduced to achieve local and global consistency in the graph domain [50, 51], and was then generalized to hypergraphs [52, 8]. Zhou et al. [52] propose a regularization function by reducing the higher-order structure using clique expansion. To directly utilize the higher-order structures, Hein et al. [53] propose a regularization function based on the total variation of the hypergraph. Other regularization functions are designed to improve parallelization ability and introduce non-linearity [54, 55, 24, 22]. To efficiently calculate the diffusion process when using complex regularization functions, some advanced optimization techniques have been investigated [56, 57]. While hypergraph diffusion methods have shown effectiveness in various tasks like ranking, motif clustering, and signal processing [58, 25, 59, 60], they are all restricted to node representations and cannot address the ENC problem.

In this paper, we extend hypergraph diffusion using node-hyperedge co-representations and parameterize this process using neural networks, resulting in a novel HGNN architecture. Most related to our work is ED-HNN [20], which presents a neural implementation for the traditional hypergraph diffusion. However, their method is based on message passing, which still suffers from the three limitations discussed in the introduction. Instead, we introduce co-representations and model both within-edge and within-node interactions as multi-input multi-output functions, which effectively tackles these limitations and demonstrates significant improvements in our experiments.

3 Preliminaries

Notations. Let $\mathcal{G} = (\mathcal{V}, \mathcal{E})$ denote a hypergraph, where $\mathcal{V} = \{v_1, v_2, \dots, v_n\}$ represents a set of n nodes, and $\mathcal{E} = \{e_1, e_2, \dots, e_m\}$ represents a set of m hyperedges. Each hyperedge $e_i \in \mathcal{E}$ is a non-empty subset of \mathcal{V} and can contain an arbitrary number of nodes. $\mathcal{E}_v = \{e \in \mathcal{E} | v \in e\}$ represents the set of hyperedges that contain node v , and $d_v = |\mathcal{E}_v|$ and $d_e = |e|$ are the degrees of node v and hyperedge e , respectively. We use v_i^e and e_j^v to denote the i -th node in hyperedge e and the j -th hyperedge in \mathcal{E}_v . $\mathbf{X}^{(0)} = [\mathbf{x}_{v_1}^{(0)}, \dots, \mathbf{x}_{v_n}^{(0)}]^\top$ is the initial node feature matrix.

Message Passing-based HGNNs. The two-stage message passing framework [18, 40], which can represent most existing HGNNs, is formulated as:

$$\mathbf{z}_e^{(t+1)} = f_{\mathcal{V} \rightarrow \mathcal{E}}(\mathbf{X}_e^{(t)}; \mathbf{z}_e^{(t)}), \quad (1)$$

$$\tilde{\mathbf{x}}_v^{(t+1)} = f_{\mathcal{E} \rightarrow \mathcal{V}}(\mathbf{Z}_v^{(t+1)}; \mathbf{x}_v^{(t)}), \quad (2)$$

$$\mathbf{x}_v^{(t+1)} = f_{\text{skip}}(\tilde{\mathbf{x}}_v^{(t+1)}, \mathbf{x}_v^{(t)}, \mathbf{x}_v^{(0)}). \quad (3)$$

Here $\mathbf{x}_v^{(t)}$ and $\mathbf{z}_e^{(t)}$ are the node and hyperedge representations in the (t) -th iteration. $\mathbf{z}_e^{(0)}$ is typically initialized by a zero vector or the mean vector of the node features. $\mathbf{X}_e^{(t)}$ denotes the representations of nodes contained in hyperedge e , i.e., $\mathbf{X}_e^{(t)} = [\mathbf{x}_{v_1^e}^{(t)}, \dots, \mathbf{x}_{v_{d_e}^e}^{(t)}]^\top$. Similarly, $\mathbf{Z}_v^{(t)} = [\mathbf{z}_{e_1^v}^{(t)}, \dots, \mathbf{z}_{e_{d_v}^v}^{(t)}]^\top$ denotes the representations of hyperedges containing node v . $f_{\mathcal{V} \rightarrow \mathcal{E}}$ and $f_{\mathcal{E} \rightarrow \mathcal{V}}$ take multiple representations from neighboring nodes or hyperedges as inputs, and output a single hyperedge or node representation. Eq. 3 represents the optional skip connection of the original features, which can help mitigate the over-smoothing issue [18].

Hypergraph Diffusion. Hypergraph diffusion learns all node representations $\mathcal{X} = [\mathbf{x}_{v_1}, \dots, \mathbf{x}_{v_n}]^\top$, where $\mathbf{x}_{v_i} \in \mathbb{R}^d$, by the gradients of some regularization functions [24, 61]. These regularization functions are also referred to as potential functions or energy functions [20, 62], which are predefined without trainable weights. We use $\mathbf{X}_e = [\mathbf{x}_{v_1^e}, \dots, \mathbf{x}_{v_{d_e}^e}]^\top$ to denote the representations of nodes contained in a hyperedge e .

Definition 1 (Node-Representation Hypergraph Diffusion). *Given non-structural regularization functions $\mathcal{R}_v(\cdot; \mathbf{a}_v) : \mathbb{R}^d \rightarrow \mathbb{R}$ and edge regularization functions $\Omega_e(\cdot) : \mathbb{R}^{d_e \times d} \rightarrow \mathbb{R}$, the node-representation hypergraph diffusion learns representations by solving the following problem*

$$\mathcal{X}^* = \arg \min_{\mathcal{X}} \sum_{v \in \mathcal{V}} \mathcal{R}_v(\mathbf{x}_v; \mathbf{a}_v) + \lambda \sum_{e \in \mathcal{E}} \Omega_e(\mathbf{X}_e). \quad (4)$$

The non-structural regularization function $\mathcal{R}_v(\cdot; \mathbf{a}_v)$ is independent of the hypergraph structure, which is commonly defined as the squared loss function [52, 61]. \mathbf{a}_v is the node attribute vector (composed of node features [25] or observed node labels [24]). Many structural regularization functions are proposed to implement the edge regularization functions $\Omega_e(\cdot)$ [52–55]. For example, the clique expansion (CE) regularization functions [52], defined as $\Omega_{\text{CE}}(\mathbf{X}_e) := \sum_{v, u \in e} \|\mathbf{x}_v - \mathbf{x}_u\|_2^2$, tend to force all the node representations in a hyperedge to become similar.

4 Methodology

4.1 Co-Representation Hypergraph Diffusion

In this section, we extend the current hypergraph diffusion concept using co-representations of node-hyperedge pairs. This extension enables its application in addressing the ENC problem [12].

Problem 1 (Edge-Dependent Node Classification (ENC)). *Given (1) a hypergraph $\mathcal{G} = (\mathcal{V}, \mathcal{E})$, (2) observed edge-dependent node labels in $\mathcal{E}' \subset \mathcal{E}$ (i.e., $y_{v,e}, \forall v \in e, \forall e \in \mathcal{E}'$), and (3) an initial node feature matrix $\mathbf{X}^{(0)}$ (optional), the ENC problem is to predict the unobserved edge-dependent node labels in $\mathcal{E} \setminus \mathcal{E}'$ (i.e., $y_{v,e}, \forall v \in e, \forall e \in \mathcal{E} \setminus \mathcal{E}'$).*

In ENC, the label $y_{v,e}$ is associated with both the node v and the hyperedge e . Therefore, we extend hypergraph diffusion to learn a co-representation $\mathbf{h}_{v,e} \in \mathbb{R}^d$ for each node-hyperedge pair (v, e) . We name this co-representation hypergraph diffusion. Let $\mathcal{H} = [\dots, \mathbf{h}_{v,e}, \dots]^\top$ denote the collection of all co-representation vectors. We use $\mathbf{H}_e = [\mathbf{h}_{v_1^e, e}, \dots, \mathbf{h}_{v_{d_e}^e, e}]^\top$ and $\mathbf{H}_v = [\mathbf{h}_{v, e_1^v}, \dots, \mathbf{h}_{v, e_{d_v}^v}]^\top$ to represent the co-representations associated with a hyperedge e or a node v , respectively.

Definition 2 (Co-Representation Hypergraph Diffusion). *Given non-structural regularization functions $\mathcal{R}_{v,e}(\cdot; \mathbf{x}_v) : \mathbb{R}^d \rightarrow \mathbb{R}$, edge regularization functions $\Omega_e(\cdot) : \mathbb{R}^{d_e \times d} \rightarrow \mathbb{R}$, and node regularization functions $\Omega_v(\cdot) : \mathbb{R}^{d_v \times d} \rightarrow \mathbb{R}$, the co-representation hypergraph diffusion learns representations by solving the following optimization problem*

$$\mathcal{H}^* = \arg \min_{\mathcal{H}} \sum_{v \in \mathcal{V}} \sum_{e \in \mathcal{E}_v} \mathcal{R}_{v,e}(\mathbf{h}_{v,e}; \mathbf{a}_{v,e}) + \lambda \sum_{e \in \mathcal{E}} \Omega_e(\mathbf{H}_e) + \gamma \sum_{v \in \mathcal{V}} \Omega_v(\mathbf{H}_v). \quad (5)$$

Here $\mathcal{R}_{v,e}(\cdot; \mathbf{a}_{v,e})$ is independent of the hypergraph structure, where $\mathbf{a}_{v,e}$ can be any related attributes of the node-hyperedge pair (v, e) (e.g., node features, hyperedge features, or observed edge-dependent node labels). $\Omega_e(\cdot)$ and $\Omega_v(\cdot)$ represents regularization for co-representations associated with the same node or hyperedge, which can be implemented using the structural regularization functions as in traditional node-representation hypergraph diffusion [52–55].

Depending on whether the regularization functions are differentiable, we can solve Eq. 5 using one of two standard optimization methods: gradient descent (GD) or alternating direction method of multipliers (ADMM) [63]. When the regularization functions are differentiable, we first initialize $\mathbf{h}_{v,e}^{(0)} = \mathbf{a}_{v,e}$, and then solve it using GD with a step size α :

$$\mathbf{h}_{v,e}^{(t+1)} = \mathbf{h}_{v,e}^{(t)} - \alpha (\nabla \mathcal{R}_{v,e}(\mathbf{h}_{v,e}^{(t)}; \mathbf{a}_{v,e}) + \lambda [\nabla \Omega_e(\mathbf{H}_e^{(t)})]_v + \gamma [\nabla \Omega_v(\mathbf{H}_v^{(t)})]_e), \quad (6)$$

where ∇ is the gradient operator. $[\cdot]_v$ and $[\cdot]_e$ represent the gradient vector associated with node v and hyperedge e , respectively. For example, $[\nabla \Omega_e(\mathbf{H}_e^{(t)})]_v$ represents the gradient w.r.t. $\mathbf{h}_{v,e}^{(t)}$.

When the regularization functions are not all differentiable (e.g., the total variation (TV) regularization functions [53] or the Lovász extension cardinality-based (LEC) regularization functions [54]), we can apply ADMM to find the optimal solution. We first introduce auxiliary variables \mathbf{U}_e and \mathbf{Z}_v for each hyperedge and node, respectively. All variables are initialized as $\mathbf{h}_{v,e}^{(0)} = \mathbf{a}_{v,e}$, $\mathbf{U}_e^{(0)} = \mathbf{H}_e^{(0)}$, and $\mathbf{Z}_v^{(0)} = \mathbf{H}_v^{(0)}$, and then updated iteratively as follows:

$$\mathbf{U}_e^{(t+1)} = \text{prox}_{\lambda \Omega_e / \rho} (2\mathbf{H}_e^{(t)} - \mathbf{U}_e^{(t)}) + \mathbf{U}_e^{(t)} - \mathbf{H}_e^{(t)}, \quad (7)$$

$$\mathbf{Z}_v^{(t+1)} = \text{prox}_{\gamma \Omega_v / \rho} (2\mathbf{H}_v^{(t)} - \mathbf{Z}_v^{(t)}) + \mathbf{Z}_v^{(t)} - \mathbf{H}_v^{(t)}, \quad (8)$$

$$\mathbf{h}_{v,e}^{(t+1)} = \text{prox}_{\mathcal{R}_{v,e}(\cdot; \mathbf{a}_{v,e}) / 2\rho} \left(\frac{1}{2} ([\mathbf{U}_e^{(t+1)}]_v + [\mathbf{Z}_v^{(t+1)}]_e) \right). \quad (9)$$

Here $\text{prox}_g(\mathbf{H}) := \arg \min_{\mathbf{H}'} (g(\mathbf{H}') + \frac{1}{2} \|\mathbf{H}' - \mathbf{H}\|_F^2)$ is the proximity operator [63] in the ADMM method. The proximity operator of a lower semi-continuous convex function is 1-Lipschitz continuous [64], enabling its approximation by neural networks. ρ is the scaling factor in the ADMM method. We leave the derivation of Eq. 7-9 to Appendix D.1.

$\nabla \Omega_e(\cdot)$ or $\text{prox}_{\lambda \Omega_e / \rho}(\cdot)$ in the GD or ADMM method are referred to as *edge diffusion operators*, which generate within-edge information that should “diffuse” to each node-hyperedge pair. In a similar way, $\nabla \Omega_v(\cdot)$ or $\text{prox}_{\gamma \Omega_v / \rho}(\cdot)$ are referred to as *node diffusion operators*.

The hyperedges and nodes are inherently unordered, hence in designing structural regularization functions it is important to ensure the outputs are consistent regardless of the input ordering. We say a function $g : \mathbb{R}^{n \times d} \rightarrow \mathbb{R}^{d'}$ is permutation invariant, if for any action π from the row permutation group \mathbb{S}_n , it holds that $g(\pi \cdot \mathbf{H}) = g(\mathbf{H})$ for all $\mathbf{H} \in \mathbb{R}^{n \times d}$. Similarly, function $g : \mathbb{R}^{n \times d} \rightarrow \mathbb{R}^{n \times d'}$ is permutation equivariant, if for any $\pi \in \mathbb{S}_n$, it holds that $g(\pi \cdot \mathbf{H}) = \pi \cdot g(\mathbf{H})$ for all $\mathbf{H} \in \mathbb{R}^{n \times d}$. Existing structural regularization functions are shown to be permutation invariant [20].

Proposition 1 (Wang et al. [20]). *With permutation invariant structural regularization functions, the diffusion operators are permutation equivariant.*

Proposition 1 shows that the edge and node diffusion operators are permutation equivariant. This critical property enables the modeling of complex interactions as multi-input multi-output functions while ensuring the outputs can commute according to the input ordering.

Next, we show that the proposed co-representation hypergraph diffusion is a more general concept than node-representation hypergraph diffusion.

Proposition 2. *The node-representation hypergraph diffusion is a special case of the co-representation hypergraph diffusion.*

We leave all the proofs to Appendix D. Node-representation hypergraph diffusion is equivalent to imposing a strict constraint that all the co-representations associated with the same node must be identical, resulting in a single unified node representation. Instead, co-representation hypergraph diffusion relaxes this constraint by introducing node regularization functions, which enables multiple co-representations associated with the same node to be different.

4.2 Co-representation Neural Hypergraph Diffusion

In this section, we propose **CoNHD** (**Co**-representation **N**eural **H**ypergraph **D**iffusion), a neural implementation of the co-representation hypergraph diffusion process, which can easily adapt to different ENC datasets. This implementation naturally leads to the novel and effective HGNN architecture illustrated in Fig. 1(d).

Equivariant Neural Diffusion Operators. Compared to the invariant aggregation operators in message passing, the equivariant diffusion operators in hypergraph diffusion can generate diverse diffusing information that is specific to each node-hyperedge pair. Since nodes and hyperedges are inherently unordered, the equivariance property of diffusion operators is crucial for modeling multi-input multi-output interactions, which ensures that the output for each node-hyperedge pair remains consistent regardless of the input ordering. However, traditional diffusion operators rely on handcrafting structural regularization functions, which is challenging and requires good insights of the datasets. To mitigate this challenge, we use set-equivariant neural networks to parameterize the edge and node diffusion operators, denoted as $\phi(\cdot)$ and $\varphi(\cdot)$, which can be trained in a data-driven manner while preserving the equivariance property. Apart from the unweighted pooling-based implementation explored in [20], we also consider an implementation based on self-attention, which has shown practical effectiveness in many real-world applications [65, 12].

UNweighted Pooling (UNP). Unweighted pooling is widely investigated for implementing set-equivariant neural networks [66–68]. Wang et al. [20] provide an implementation and show its effectiveness in approximating the node-representation hypergraph diffusion process. As it utilizes an unweighted sum pooling to aggregate global set information, we refer to this implementation as UNweighted Pooling. The UNP implementation can be represented as follows:

$$\text{UNP: } [\text{UNP}(\mathbf{H})]_i = \text{MLP}\left(\left[h_i, \sum_{h_j \in \mathbf{H}} \text{MLP}(h_j)\right]\right). \quad (10)$$

Here $\mathbf{H} \in \mathbb{R}^{n_H \times d}$ represents a matrix with n_H co-representation vectors, which can be replaced by \mathbf{H}_e or \mathbf{H}_v according to the inputs of the diffusion operators. $\text{MLP}(\cdot)$ is a Multi-Layer Perceptron (MLP). This simple implementation can approximate **any** continuous permutation equivariant functions [20], leading to a universal approximator for our diffusion operators. Besides, its time complexity is linear to the number of the input co-representations.

Induced Set Attention Block (ISAB). The static unweighted sum pooling operation ignores the importance of different elements, limiting its ability to capture interactions in practice [69–71]. Therefore, we consider another implementation using Set Transformer [69], which is based on self-attention. Different from other HGNNs that employ the invariant aggregation (single-output) module of Set Transformer [40, 12], our approach relies solely on the permutation equivariant module ISAB to implement the multi-input multi-output diffusion operators:

$$\begin{aligned} \text{ISAB: } \quad & \text{ISAB}(\mathbf{H}) = \text{MAB}(\mathbf{H}, \text{MAB}(\mathbf{I}, \mathbf{H})), \\ \text{where } \quad & \text{MAB}(\mathbf{Q}, \mathbf{K}) = \text{LN}(\mathbf{M} + \text{RFF}(\mathbf{M})), \mathbf{M} = \text{LN}(\mathbf{Q}, \text{MULTIHEAD}(\mathbf{Q}, \mathbf{K}, \mathbf{K})), \\ & \text{MULTIHEAD}(\mathbf{Q}, \mathbf{K}, \mathbf{V}) = [\mathbf{O}_1, \dots, \mathbf{O}_h] \cdot \mathbf{W}^O, \\ & \mathbf{O}_i = \omega(\mathbf{Q}\mathbf{W}_i^Q (\mathbf{K}\mathbf{W}_i^K)^\top) \mathbf{V}\mathbf{W}_i^V. \end{aligned} \quad (11)$$

Here \mathbf{I} , \mathbf{W}^O , \mathbf{W}^Q , \mathbf{W}^K , and \mathbf{W}^V are all trainable weights. $\text{LN}(\cdot)$ denotes the layer normalization. $\text{RFF}(\cdot)$ is a row-wise feed-forward layer. $\text{MULTIHEAD}(\cdot)$ is the multihead attention mechanism and ω is the softmax function. ISAB utilizes a fixed number of inducing points $\mathbf{I} \in \mathbb{R}^{k \times d}$ to reduce the quadratic complexity in self attention to linear complexity [69], which can increase the efficiency when modeling hypergraphs with larger node and hyperedge degrees.

Co-representation Neural Hypergraph Diffusion. We build a neural implementation for the co-representation hypergraph diffusion process using two neural diffusion operators ϕ and φ . Following the update rules of the GD or ADMM optimization in Eq. 6 or Eq. 7-9, we provide two

implementations of our model architecture. The $(t + 1)$ -th layer can be represented as:

$$\text{GD-based: } \mathbf{M}_e^{(t+1)} = \phi(\mathbf{H}_e^{(t)}), \mathbf{M}_v^{(t+1)} = \varphi(\mathbf{H}_v^{(t)}), \quad (12)$$

$$\mathbf{h}_{v,e}^{(t+1)} = \psi([\mathbf{h}_{v,e}^{(t)}, \mathbf{m}_{v,e}^{(t+1)}, \mathbf{m}_{v,e}'^{(t+1)}, \mathbf{h}_{v,e}^{(0)}]), \quad (13)$$

$$\text{ADMM-based: } \mathbf{M}_e^{(t+1)} = \phi(2\mathbf{H}_e^{(t)} - \mathbf{M}_e^{(t)}) + \mathbf{M}_e^{(t)} - \mathbf{H}_e^{(t)}, \quad (14)$$

$$\mathbf{M}_v^{(t+1)} = \varphi(2\mathbf{H}_v^{(t)} - \mathbf{M}_v^{(t)}) + \mathbf{M}_v^{(t)} - \mathbf{H}_v^{(t)}, \quad (15)$$

$$\mathbf{h}_{v,e}^{(t+1)} = \psi([\mathbf{m}_{v,e}^{(t+1)}, \mathbf{m}_{v,e}'^{(t+1)}, \mathbf{h}_{v,e}^{(0)}]). \quad (16)$$

Here $\mathbf{M}_e^{(t)} = [\mathbf{m}_{v_1^e, e}^{(t)}, \dots, \mathbf{m}_{v_{d_e}^e, e}^{(t)}]^\top$ and $\mathbf{M}_v^{(t)} = [\mathbf{m}_{v, e_1^v}^{(t)}, \dots, \mathbf{m}_{v, e_{d_v}^v}^{(t)}]$ are the within-edge and within-node diffusing information generated using the neural diffusion operators ϕ and φ , which are implemented as either UNP (Eq. 10) or ISAB (Eq. 11). $\psi(\cdot)$ collects the diffusing information and updates the co-representation vectors. In our experiments, we implement $\psi(\cdot)$ as a linear layer. $\mathbf{h}_{v,e}^{(0)}$ is the initial feature vector, which corresponds to the non-structural regularization term in Eq. 5. Due to the dependency of historical auxiliary variables, the ADMM-based implementation needs to preserve the historical diffusing information $\mathbf{M}_e^{(t)}$ and $\mathbf{M}_v^{(t)}$ from the last step.

We compare the proposed CoNHD model to message passing-based HGNNs in Appendix B. We show that CoNHD is expressive enough to represent any message passing-based HGNNs. Besides, by modeling the within-edge and within-node interactions as multi-input multi-output functions, CoNHD can effectively tackle the three limitations of message passing as discussed in the introduction. Notably, despite the increased expressiveness, CoNHD still maintains high efficiency. We provide theoretical complexity analysis in Appendix F.1.

5 Experiments

5.1 Edge-Dependent Node Classification

Datasets. We conduct experiments on all six real-world ENC datasets in [12]. These datasets are Email (Email-Enron and Email-Eu), StackOverflow (Stack-Biology and Stack-Physics), and Co-authorship networks (Coauth-DBLP and Coauth-AMiner). The statistics are shown in Table 1. Notably, Email-Enron and Email-Eu have relatively large node degrees, while Email-Enron has relatively large hyperedge degrees as well. Further information can be found in Appendix G.

Baselines. We compare the GD-based CoNHD model to 9 baseline models. For CoNHD, we compare two variants with different neural diffusion operators, UNP (Eq. 10) and ISAB (Eq. 11). The baselines include 6 models following the traditional message passing framework (HNHN [38], HyperGNN [34], HCHA [36], HAT [72], UniGCNII [18], and AllSet-Transformer [40]) and 3 recent models that utilize edge-dependent node information in message passing (HNN [19], ED-HNN [20], and WHATsNet [12]). More details are provided in Appendix H.

Effectiveness. As shown in Table 2, CoNHD consistently achieves the best performance across all datasets in terms of both Micro-F1 and Macro-F1 metrics. Especially, CoNHD achieves significant improvements on Email-Enron and Email-Eu datasets (with gains of approximately 10% on Email-Enron) compared to the best baseline WHATsNet. As indicated before, the main difference between these two datasets and the others is that they have relatively large-degree nodes or hyperedges. All the baseline methods based on node or hyperedge representations can easily cause potential information loss for large degree nodes or hyperedges. In contrast, CoNHD can preserve specific information for each node-hyperedge pair using co-representations.

Table 1: Statistics of six ENC datasets.

Dataset	Num. of Nodes	Num. of Edges	Avg. d_v	Avg. d_e	Max. d_v	Max. d_e
Email-Enron	21,251	101,124	55.83	11.73	18,168	948
Email-Eu	986	209,508	549.54	2.59	8,659	59
Stack-Biology	15,490	26,823	3.63	2.10	1,318	12
Stack-Physics	80,936	200,811	5.93	2.39	6,332	48
Coauth-DBLP	108,484	91,266	2.96	3.52	236	36
Coauth-AMiner	1,712,433	2,037,605	3.03	2.55	752	115

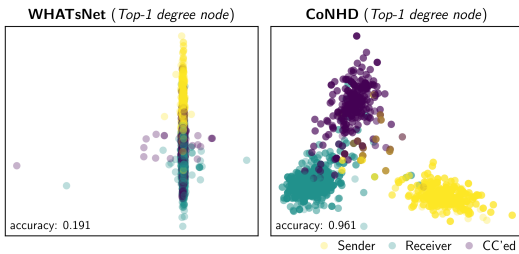


Figure 2: **Visualization of embeddings in the Email-Enron dataset using LDA.** The embeddings learned by CoNHD exhibit clearer distinctions based on the edge-dependent labels compared to the embeddings learned by WHATsNet.

Table 2: **Performance of edge-dependent node classification.** Bold numbers indicate the best results. Underlined numbers indicate the second-best results. “OOM” indicates “Out Of Memory”.

Method	Email-Enron		Email-Eu		Stack-Biology	
	Micro-F1	Macro-F1	Micro-F1	Macro-F1	Micro-F1	Macro-F1
HNHN [38]	0.738 \pm 0.028	0.637 \pm 0.023	0.643 \pm 0.004	0.552 \pm 0.014	0.640 \pm 0.005	0.592 \pm 0.006
HyperGNN [34]	0.725 \pm 0.004	0.674 \pm 0.003	0.633 \pm 0.001	0.533 \pm 0.008	0.689 \pm 0.002	0.624 \pm 0.007
HCHA [36]	0.666 \pm 0.010	0.464 \pm 0.002	0.620 \pm 0.000	0.497 \pm 0.001	0.589 \pm 0.007	0.465 \pm 0.060
HAT [72]	0.817 \pm 0.001	0.753 \pm 0.004	0.669 \pm 0.001	0.638 \pm 0.002	0.661 \pm 0.005	0.606 \pm 0.005
UniGCNII [18]	0.734 \pm 0.010	0.656 \pm 0.010	0.630 \pm 0.005	0.565 \pm 0.013	0.610 \pm 0.004	0.433 \pm 0.007
AllSetTransformer [40]	0.796 \pm 0.014	0.719 \pm 0.020	0.666 \pm 0.005	0.624 \pm 0.021	0.571 \pm 0.054	0.446 \pm 0.081
HNN [19]	0.763 \pm 0.003	0.679 \pm 0.007	OOM	OOM	0.618 \pm 0.015	0.568 \pm 0.013
ED-HNN [20]	0.778 \pm 0.001	0.713 \pm 0.004	0.648 \pm 0.001	0.558 \pm 0.004	0.688 \pm 0.005	0.506 \pm 0.002
WHATsNet [12]	0.826 \pm 0.001	0.760 \pm 0.004	0.671 \pm 0.000	0.646 \pm 0.003	0.742 \pm 0.003	0.686 \pm 0.004
CoNHD (UNP)	0.905 \pm 0.001	0.858 \pm 0.004	0.708 \pm 0.001	0.689 \pm 0.001	0.748 \pm 0.003	0.694 \pm 0.005
CoNHD (ISAB)	0.911 \pm 0.001	0.871 \pm 0.002	0.709 \pm 0.001	0.690 \pm 0.002	0.749 \pm 0.002	0.695 \pm 0.004

Method	Stack-Physics		Coauth-DBLP		Coauth-AMiner	
	Micro-F1	Macro-F1	Micro-F1	Macro-F1	Micro-F1	Macro-F1
HNHN [38]	0.506 \pm 0.053	0.422 \pm 0.043	0.486 \pm 0.004	0.478 \pm 0.008	0.520 \pm 0.002	0.514 \pm 0.002
HyperGNN [34]	0.686 \pm 0.004	0.630 \pm 0.002	0.540 \pm 0.004	0.519 \pm 0.002	0.566 \pm 0.002	0.551 \pm 0.004
HCHA [36]	0.622 \pm 0.003	0.481 \pm 0.007	0.451 \pm 0.007	0.334 \pm 0.048	0.468 \pm 0.020	0.447 \pm 0.040
HAT [72]	0.708 \pm 0.005	0.643 \pm 0.009	0.503 \pm 0.004	0.483 \pm 0.006	0.543 \pm 0.002	0.533 \pm 0.003
UniGCNII [18]	0.671 \pm 0.022	0.492 \pm 0.016	0.497 \pm 0.003	0.476 \pm 0.002	0.520 \pm 0.001	0.507 \pm 0.001
AllSetTransformer [40]	0.728 \pm 0.039	0.646 \pm 0.046	0.495 \pm 0.038	0.487 \pm 0.040	0.577 \pm 0.005	0.570 \pm 0.002
HNN [19]	0.683 \pm 0.005	0.617 \pm 0.005	0.488 \pm 0.006	0.482 \pm 0.006	0.543 \pm 0.002	0.533 \pm 0.002
ED-HNN [20]	0.726 \pm 0.002	0.617 \pm 0.006	0.514 \pm 0.016	0.484 \pm 0.024	0.503 \pm 0.006	0.479 \pm 0.008
WHATsNet [12]	0.770 \pm 0.003	0.707 \pm 0.004	0.605 \pm 0.002	0.595 \pm 0.002	0.630 \pm 0.005	0.623 \pm 0.007
CoNHD (UNP)	0.776 \pm 0.001	0.712 \pm 0.005	0.609 \pm 0.004	0.596 \pm 0.003	0.630 \pm 0.002	0.626 \pm 0.002
CoNHD (ISAB)	0.777 \pm 0.001	0.710 \pm 0.004	0.610 \pm 0.002	0.595 \pm 0.003	0.638 \pm 0.002	0.632 \pm 0.002

Besides, compared to the aggregation operation in message passing, the two equivariant neural diffusion operators in CoNHD can generate different diffusing information to different node-hyperedge pairs, which is more expressive especially when modeling interactions within a large-degree node or hyperedge. This can explain why CoNHD can achieve more improvements on the two datasets with larger node and hyperedge degrees.

The performance gap between the two neural diffusion operators in CoNHD is minimal. While the UNP operator can theoretically approximate any equivariant functions, the ISAB operator overall demonstrates better performance in our experiments. This may be attributed to the practical effectiveness of the attention mechanism, which is consistent with previous research [40].

Fig. 2 visualizes the learned embeddings of node-hyperedge pairs associated with the largest-degree node in the Email-Enron dataset using LDA. CoNHD can learn more separable embeddings than WHATsNet. We show more examples in Appendix I.1.

Efficiency. The performance and training time on Email-Enron and Email-Eu are illustrated in Fig. 3. All experiments are conducted on a single mini-NVIDIA A100 GPU. Only models using mini-NVIDIA training are considered in the comparison. HCHA and HNN are excluded as their source code is based on full-batch training, which is impractical when handling large real-world hypergraphs. The best baseline, WHATsNet, sacrifices efficiency to improve performance. In contrast, our proposed method, CoNHD, not only achieves the best performance but also maintains high efficiency. In each layer, CoNHD only incorporates direct neighbors of the node-hyperedge pairs, which can reduce the computational costs compared to message passing. We provide more analysis in Appendix F.2.

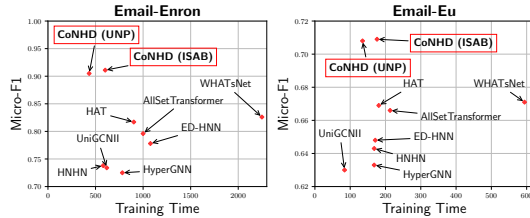


Figure 3: **Comparison of the performance and training time (minutes).** CoNHD demonstrates significant improvements in terms of Micro-F1 while maintaining good efficiency. The same conclusion holds for Macro-F1 (results not shown).

5.2 Approximation of Common Diffusion Operators

We conduct experiments to verify whether CoNHD, as a neural implementation of co-representation hypergraph diffusion, can effectively approximate common hypergraph diffusion operators.

Datasets. We use the Senate [73] dataset with the same 1-dimensional feature initialization as in [20]. Although our proposed CoNHD model can accept any input features related to the node-hyperedge pairs, we only utilize initial node features to fit the input of other baseline HGNNs. To generate the labels, we perform the co-representation hypergraph diffusion process using three common diffusion operators: CE [52], TV [53], and LEC [54]. More details can be found in Appendix G.

Baselines. We compare both ADMM-based (Eq. 14-16) and GD-based (Eq. 12-13) implementations of the proposed CoNHD model (with ISAB operator) to two baseline methods, ED-HNN [20] and WHATsNet [12]. ED-HNN is a universal approximator for any node-representation hypergraph diffusion process, while WHATsNet is the best baseline in the ENC experiments.

Results. The results in terms of Mean Absolute Error (MAE) are reported in Table 3. All methods demonstrate superior performance in approximating the invariant CE operator. Conversely, approximating the equivariant and non-differentiable operators, TV and LEC, are more challenging. The proposed method CoNHD can achieve the lowest MAE results compared to the baseline methods in all settings. While the ADMM-based implementation is theoretically more suitable for approximating non-differentiable diffusion operators, it demonstrates minimal performance differences compared to the GD-based implementation in practice.

Table 3: **MAE (\downarrow) results of approximating common diffusion operators.**

Method	CE	TV	LEC
ED-HNN [20]	0.0132 \pm 0.0028	0.0394 \pm 0.0011	0.2057 \pm 0.0004
WHATsNet [12]	0.0065 \pm 0.0019	0.0380 \pm 0.0007	0.2056 \pm 0.0014
CoNHD (ADMM)	0.0012 \pm 0.0001	0.0293 \pm 0.0000	0.0532 \pm 0.0031
CoNHD (GD)	0.0011 \pm 0.0003	0.0292 \pm 0.0001	0.0561 \pm 0.0056

5.3 Ablation Study

One critical design choice in the proposed CoNHD method is the use of equivariant instead of invariant operators, which enable the modeling of within-edge and within-node interactions as multi-input multi-output functions. To investigate the effectiveness of this choice, we replace the within-edge diffusion operator ϕ and the within-node diffusion operator φ with invariant diffusion operators. We implement the invariant operator using the same architecture as the equivariant operator but with mean aggregation applied to the final outputs, which generates the same output for different node-hyperedge pairs. The mean aggregation is widely used in most message passing-based HGNNs [18]. We conduct experiments on Email-Enron and Email-Eu, the two datasets with the largest improvements in the ENC experiments.

Table 4: **Effectiveness of the equivariance in two diffusion operators ϕ and φ .** \checkmark and \times indicate whether the corresponding operator is equivariant or invariant, respectively.

Method	ϕ	φ	Email-Enron		Email-Eu	
			Micro-F1	Macro-F1	Micro-F1	Macro-F1
CoNHD (UNP)	\times	\times	0.827 \pm 0.000	0.769 \pm 0.004	0.673 \pm 0.000	0.645 \pm 0.001
	\times	\checkmark	0.876 \pm 0.001	0.817 \pm 0.006	0.698 \pm 0.001	0.677 \pm 0.002
	\checkmark	\times	0.903 \pm 0.001	0.855 \pm 0.004	0.707 \pm 0.000	0.688 \pm 0.002
	\checkmark	\checkmark	0.905 \pm 0.001	0.858 \pm 0.004	0.708 \pm 0.001	0.689 \pm 0.001
CoNHD (ISAB)	\times	\times	0.829 \pm 0.001	0.765 \pm 0.007	0.673 \pm 0.001	0.647 \pm 0.002
	\times	\checkmark	0.878 \pm 0.001	0.823 \pm 0.005	0.698 \pm 0.001	0.678 \pm 0.003
	\checkmark	\times	0.910 \pm 0.001	0.870 \pm 0.003	0.707 \pm 0.001	0.689 \pm 0.001
	\checkmark	\checkmark	0.911 \pm 0.001	0.871 \pm 0.002	0.709 \pm 0.001	0.690 \pm 0.002

As shown in Table 4, CoNHD with two equivariant operators achieves the highest performance, exhibiting significant improvements compared to the variant with two invariant operators. Furthermore, variants with just one equivariant operator still outperform the fully invariant model. This suggests that equivariance benefits the modeling of both within-edge and within-node interactions. We also notice that the performance gap between the full equivariant model and the variant with only the equivariant within-edge operator ϕ is not significant. This might imply that within-edge interactions provide the most information for predicting the edge-dependent node labels.

6 Conclusion

In this paper, we develop CoNHD, a novel HGNN based on hypergraph diffusion. CoNHD explicitly models within-edge and within-node interactions among co-representations as multi-input multi-output functions, which can effectively address the ENC problem compared to message passing-based HGNNs. Our experiments demonstrate: (1) CoNHD achieves best performance on six real-world ENC datasets without sacrificing efficiency. (2) CoNHD can effectively approximate the co-representation hypergraph diffusion process with common diffusion operators. (3) As a critical design for implementing multi-output functions, the equivariance property of two diffusion operators is essential for performance improvements. We believe this work is a good exploration of novel HGNN architectures that go beyond the dominant two-stage message passing framework.

References

- [1] Ron Milo, Shai Shen-Orr, Shalev Itzkovitz, Nadav Kashtan, Dmitri Chklovskii, and Uri Alon. Network motifs: simple building blocks of complex networks. *Science*, 2002.
- [2] Federico Battiston, Giulia Cencetti, Iacopo Iacopini, Vito Latora, Maxime Lucas, Alice Patania, Jean-Gabriel Young, and Giovanni Petri. Networks beyond pairwise interactions: Structure and dynamics. *Physics Reports*, 2020.
- [3] Renaud Lambiotte, Martin Rosvall, and Ingo Scholtes. From networks to optimal higher-order models of complex systems. *Nature Physics*, 2019.
- [4] Yuanzhao Zhang, Maxime Lucas, and Federico Battiston. Higher-order interactions shape collective dynamics differently in hypergraphs and simplicial complexes. *Nature Communications*, 2023.
- [5] Claude Berge. *Hypergraphs: combinatorics of finite sets*. Elsevier, 1984.
- [6] Alain Bretto. *Hypergraph theory*. Springer, 2013.
- [7] Yue Gao, Zizhao Zhang, Haojie Lin, Xibin Zhao, Shaoyi Du, and Changqing Zou. Hypergraph learning: Methods and practices. *IEEE Transactions on Pattern Analysis and Machine Intelligence*, 2020.
- [8] Alessia Antelmi, Gennaro Cordasco, Mirko Polato, Vittorio Scarano, Carmine Spagnuolo, and Dingqi Yang. A survey on hypergraph representation learning. *ACM Computing Surveys*, 2023.
- [9] Ke Tu, Peng Cui, Xiao Wang, Fei Wang, and Wenwu Zhu. Structural deep embedding for hyper-networks. In *Proceedings of the AAAI Conference on Artificial Intelligence*, 2018.
- [10] Ruochi Zhang, Yuesong Zou, and Jian Ma. Hyper-sagnn: a self-attention based graph neural network for hypergraphs. In *International Conference on Learning Representations*, 2020.
- [11] Jaehyeong Jo, Jinheon Baek, Seul Lee, Dongki Kim, Minki Kang, and Sung Ju Hwang. Edge representation learning with hypergraphs. In *Advances in Neural Information Processing Systems*, 2021.
- [12] Minyoung Choe, Sunwoo Kim, Jaemin Yoo, and Kijung Shin. Classification of edge-dependent labels of nodes in hypergraphs. In *Proceedings of the 29th ACM SIGKDD Conference on Knowledge Discovery and Data Mining*, 2023.
- [13] Jianbo Li, Jingrui He, and Yada Zhu. E-tail product return prediction via hypergraph-based local graph cut. In *Proceedings of the 24th ACM SIGKDD International Conference on Knowledge Discovery & Data Mining*, 2018.
- [14] Uthsav Chitra and Benjamin Raphael. Random walks on hypergraphs with edge-dependent vertex weights. In *International Conference on Machine Learning*, 2019.
- [15] Koby Hayashi, Sinan G Aksoy, Cheong Hee Park, and Haesun Park. Hypergraph random walks, laplacians, and clustering. In *Proceedings of the 29th ACM International Conference on Information & Knowledge Management*, 2020.
- [16] Geon Lee, Minyoung Choe, and Kijung Shin. Hashnwalk: Hash and random walk based anomaly detection in hyperedge streams. In *Proceedings of the Thirty-First International Joint Conference on Artificial Intelligence*, 2022.
- [17] Devanshu Arya, Deepak K Gupta, Stevan Rudinac, and Marcel Worring. Hypersage: Generalizing inductive representation learning on hypergraphs. *arXiv preprint arXiv:2010.04558*, 2020.
- [18] Jing Huang and Jie Yang. Unignn: a unified framework for graph and hypergraph neural networks. In *Proceedings of the Thirtieth International Joint Conference on Artificial Intelligence*, 2021.
- [19] Ryan Aponte, Ryan A Rossi, Shunan Guo, Jane Hoffswell, Nedim Lipka, Chang Xiao, Gromit Chan, Eunye Koh, and Nesreen Ahmed. A hypergraph neural network framework for learning hyperedge-dependent node embeddings. *arXiv preprint arXiv:2212.14077*, 2022.
- [20] Peihao Wang, Shenghao Yang, Yunyu Liu, Zhangyang Wang, and Pan Li. Equivariant hypergraph diffusion neural operators. In *International Conference on Learning Representations*, 2023.
- [21] Xiaobing Pei, Rongping Ye, Haoran Yang, and Ruiqi Wang. Hyperedge interaction-aware hypergraph neural network. *arXiv preprint arXiv:2401.15587*, 2024.

- [22] Meng Liu, Nate Veldt, Haoyu Song, Pan Li, and David F Gleich. Strongly local hypergraph diffusions for clustering and semi-supervised learning. In *Proceedings of the Web Conference*, 2021.
- [23] Kimon Fountoulakis, Pan Li, and Shenghao Yang. Local hyper-flow diffusion. In *Advances in Neural Information Processing Systems*, 2021.
- [24] Francesco Tudisco, Austin R Benson, and Konstantin Prokophchik. Nonlinear higher-order label spreading. In *Proceedings of the Web Conference*, 2021.
- [25] Yuuki Takai, Atsushi Miyauchi, Masahiro Ikeda, and Yuichi Yoshida. Hypergraph clustering based on pagerank. In *Proceedings of the 26th ACM SIGKDD International Conference on Knowledge Discovery & Data Mining*, 2020.
- [26] Risi Imre Kondor and John Lafferty. Diffusion kernels on graphs and other discrete structures. In *International Conference on Machine Learning*, 2002.
- [27] Ben Chamberlain, James Rowbottom, Maria I Gorinova, Michael Bronstein, Stefan Webb, and Emanuele Rossi. Grand: Graph neural diffusion. In *International Conference on Machine Learning*, 2021.
- [28] Thomas N. Kipf and Max Welling. Semi-supervised classification with graph convolutional networks. In *International Conference on Learning Representations*, 2017.
- [29] Zonghan Wu, Shirui Pan, Fengwen Chen, Guodong Long, Chengqi Zhang, and S Yu Philip. A comprehensive survey on graph neural networks. *IEEE Transactions on Neural Networks and Learning Systems*, 2020.
- [30] Shiwen Wu, Fei Sun, Wentao Zhang, Xu Xie, and Bin Cui. Graph neural networks in recommender systems: a survey. *ACM Computing Surveys*, 2022.
- [31] Sunwoo Kim, Soo Yong Lee, Yue Gao, Alessia Antelmi, Mirko Polato, and Kijung Shin. A survey on hypergraph neural networks: an in-depth and step-by-step guide. *arXiv preprint arXiv:2404.01039*, 2024.
- [32] Iulia Duta, Giulia Cassarà, Fabrizio Silvestri, and Pietro Lio. Sheaf hypergraph networks. In *Advances in Neural Information Processing Systems*, 2023.
- [33] Jielong Yan, Yifan Feng, Shihui Ying, and Yue Gao. Hypergraph dynamic system. In *International Conference on Learning Representations*, 2024.
- [34] Yifan Feng, Haoxuan You, Zizhao Zhang, Rongrong Ji, and Yue Gao. Hypergraph neural networks. In *Proceedings of the AAAI Conference on Artificial Intelligence*, 2019.
- [35] Yue Gao, Yifan Feng, Shuyi Ji, and Rongrong Ji. Hgnn+: General hypergraph neural networks. *IEEE Transactions on Pattern Analysis and Machine Intelligence*, 2022.
- [36] Song Bai, Feihu Zhang, and Philip HS Torr. Hypergraph convolution and hypergraph attention. *Pattern Recognition*, 2021.
- [37] Naganand Yadati, Madhav Nimishakavi, Prateek Yadav, Vikram Nitin, Anand Louis, and Partha Talukdar. Hypergcn: A new method for training graph convolutional networks on hypergraphs. In *Advances in Neural Information Processing Systems*, 2019.
- [38] Yihe Dong, Will Sawin, and Yoshua Bengio. Hnhn: Hypergraph networks with hyperedge neurons. In *ICML Graph Representation Learning and Beyond Workshop*, 2020.
- [39] Kaize Ding, Jianling Wang, Jundong Li, Dingcheng Li, and Huan Liu. Be more with less: Hypergraph attention networks for inductive text classification. In *Proceedings of the Conference on Empirical Methods in Natural Language Processing*, 2020.
- [40] Eli Chien, Chao Pan, Jianhao Peng, and Olgica Milenkovic. You are allset: A multiset function framework for hypergraph neural networks. In *International Conference on Learning Representations*, 2022.
- [41] Lev Telyatnikov, Maria Sofia Bucarelli, Guillermo Bernardez, Olga Zaghen, Simone Scardapane, and Pietro Lio. Hypergraph neural networks through the lens of message passing: a common perspective to homophily and architecture design. *arXiv preprint arXiv:2310.07684*, 2023.
- [42] Zexi Liu, Bohan Tang, Ziyuan Ye, Xiaowen Dong, Siheng Chen, and Yanfeng Wang. Hypergraph transformer for semi-supervised classification. In *IEEE International Conference on Acoustics, Speech and Signal Processing*, 2024.

- [43] Minhao Zou, Zhongxue Gan, Yutong Wang, Junheng Zhang, Dongyan Sui, Chun Guan, and Siyang Leng. Unig-encoder: A universal feature encoder for graph and hypergraph node classification. *Pattern Recognition*, 2024.
- [44] Tatyana Benko, Martin Buck, Ilya Amburg, Stephen J Young, and Sinan G Aksoy. Hypermagnet: A magnetic laplacian based hypergraph neural network. *arXiv preprint arXiv:2402.09676*, 2024.
- [45] Jaehyuk Yi and Jinkyoo Park. Hypergraph convolutional recurrent neural network. In *Proceedings of the 26th ACM SIGKDD International Conference on Knowledge Discovery & Data Mining*, 2020.
- [46] Zongjiang Shang and Ling Chen. Mshyper: Multi-scale hypergraph transformer for long-range time series forecasting. *arXiv preprint arXiv:2401.09261*, 2024.
- [47] Can Chen, Chen Liao, and Yang-Yu Liu. Teasing out missing reactions in genome-scale metabolic networks through hypergraph learning. *Nature Communications*, 2023.
- [48] Xuan Liu, Congzhi Song, Shichao Liu, Menglu Li, Xionghui Zhou, and Wen Zhang. Multi-way relation-enhanced hypergraph representation learning for anti-cancer drug synergy prediction. *Bioinformatics*, 2022.
- [49] David F Gleich and Michael W Mahoney. Using local spectral methods to robustify graph-based learning algorithms. In *Proceedings of the 21th ACM SIGKDD International Conference on Knowledge Discovery and Data Mining*, 2015.
- [50] Xiaojin Zhu, Zoubin Ghahramani, and John D Lafferty. Semi-supervised learning using gaussian fields and harmonic functions. In *International Conference on Machine learning*, 2003.
- [51] Dengyong Zhou, Olivier Bousquet, Thomas Lal, Jason Weston, and Bernhard Schölkopf. Learning with local and global consistency. In *Advances in Neural Information Processing Systems*, 2003.
- [52] Dengyong Zhou, Jiayuan Huang, and Bernhard Schölkopf. Learning with hypergraphs: Clustering, classification, and embedding. In *Advances in Neural Information Processing Systems*, 2007.
- [53] Matthias Hein, Simon Setzer, Leonardo Jost, and Syama Sundar Rangapuram. The total variation on hypergraphs-learning on hypergraphs revisited. In *Advances in Neural Information Processing Systems*, 2013.
- [54] Stefanie Jegelka, Francis Bach, and Suvrit Sra. Reflection methods for user-friendly submodular optimization. In *Advances in Neural Information Processing Systems*, 2013.
- [55] Francesco Tudisco, Konstantin Prokopchik, and Austin R Benson. A nonlinear diffusion method for semi-supervised learning on hypergraphs. *arXiv preprint arXiv:2103.14867*, 2021.
- [56] Chenzi Zhang, Shuguang Hu, Zhihao Gavin Tang, and TH Hubert Chan. Re-revisiting learning on hypergraphs: confidence interval and subgradient method. In *International Conference on Machine Learning*, 2017.
- [57] Pan Li, Niao He, and Olgica Milenkovic. Quadratic decomposable submodular function minimization: Theory and practice. *The Journal of Machine Learning Research*, 2020.
- [58] Pan Li and Olgica Milenkovic. Inhomogeneous hypergraph clustering with applications. In *Advances in Neural Information Processing Systems*, 2017.
- [59] Songyang Zhang, Zhi Ding, and Shuguang Cui. Introducing hypergraph signal processing: Theoretical foundation and practical applications. *IEEE Internet of Things Journal*, 2019.
- [60] Michael T Schaub, Yu Zhu, Jean-Baptiste Seby, T Mitchell Roddenberry, and Santiago Segarra. Signal processing on higher-order networks: Livin’ on the edge... and beyond. *Signal Processing*, 2021.
- [61] Konstantin Prokopchik, Austin R Benson, and Francesco Tudisco. Nonlinear feature diffusion on hypergraphs. In *International Conference on Machine Learning*, 2022.
- [62] Yuxin Wang, Quan Gan, Xipeng Qiu, Xuanjing Huang, and David Wipf. From hypergraph energy functions to hypergraph neural networks. In *International Conference on Machine Learning*, 2023.
- [63] Stephen Boyd, Neal Parikh, Eric Chu, Borja Peleato, Jonathan Eckstein, et al. Distributed optimization and statistical learning via the alternating direction method of multipliers. *Foundations and Trends® in Machine learning*, 2011.

- [64] Neal Parikh, Stephen Boyd, et al. Proximal algorithms. *Foundations and trends® in Optimization*, 2014.
- [65] Ashkan Shahbazi, Abihith Kothapalli, Xinran Liu, Robert Sheng, and Soheil Kolouri. Equivariant vs. invariant layers: A comparison of backbone and pooling for point cloud classification. *arXiv preprint arXiv:2306.05553*, 2023.
- [66] Manzil Zaheer, Satwik Kottur, Siamak Ravanbakhsh, Barnabas Poczos, Russ R Salakhutdinov, and Alexander J Smola. Deep sets. In *Advances in Neural Information Processing Systems*, 2017.
- [67] Charles R Qi, Hao Su, Kaichun Mo, and Leonidas J Guibas. Pointnet: Deep learning on point sets for 3d classification and segmentation. In *Proceedings of the IEEE Conference on Computer Vision and Pattern Recognition*, 2017.
- [68] Nimrod Segol and Yaron Lipman. On universal equivariant set networks. In *International Conference on Learning Representations*, 2020.
- [69] Juho Lee, Yoonho Lee, Jungtaek Kim, Adam Kosiosek, Seungjin Choi, and Yee Whye Teh. Set transformer: A framework for attention-based permutation-invariant neural networks. In *International Conference on Machine Learning*, 2019.
- [70] Jinwoo Kim, Saeyoon Oh, and Seunghoon Hong. Transformers generalize deepsets and can be extended to graphs & hypergraphs. In *Advances in Neural Information Processing Systems*, 2021.
- [71] Jinwoo Kim, Saeyoon Oh, Sungjun Cho, and Seunghoon Hong. Equivariant hypergraph neural networks. In *European Conference on Computer Vision*, 2022.
- [72] Hyunjin Hwang, Seungwoo Lee, and Kijung Shin. Hyfer: A framework for making hypergraph learning easy, scalable and benchmarkable. In *WWW Workshop on Graph Learning Benchmarks*, 2021.
- [73] James H Fowler. Legislative cosponsorship networks in the us house and senate. *Social networks*, 2006.
- [74] Hao Yuan, Haiyang Yu, Shurui Gui, and Shuiwang Ji. Explainability in graph neural networks: A taxonomic survey. *IEEE Transactions on Pattern Analysis and Machine Intelligence*, 2022.
- [75] Phillip E Pope, Soheil Kolouri, Mohammad Rostami, Charles E Martin, and Heiko Hoffmann. Explainability methods for graph convolutional neural networks. In *Proceedings of the IEEE Conference on Computer Vision and Pattern Recognition*, 2019.
- [76] Hyosoon Jang, Seonghyun Park, Sangwoo Mo, and Sungsoo Ahn. Diffusion probabilistic models for structured node classification. In *Advances in Neural Information Processing Systems*, 2023.
- [77] Chaoqi Yang, Ruijie Wang, Shuochao Yao, and Tarek Abdelzaher. Semi-supervised hypergraph node classification on hypergraph line expansion. In *Proceedings of the 31st ACM International Conference on Information & Knowledge Management*, 2022.
- [78] Özgür Yeniay. Penalty function methods for constrained optimization with genetic algorithms. *Mathematical and Computational Applications*, 2005.
- [79] Ashwin Paranjape, Austin R Benson, and Jure Leskovec. Motifs in temporal networks. In *Proceedings of the tenth ACM international conference on web search and data mining*, 2017.
- [80] Agarwal Swati, S Ashish, M Nitish, K Rohan, and C Denzil. Db1p records and entries for key computer science conferences, 2017.

Appendix

Contents

A	Broader Impacts and Limitations	14
B	Comparison to Message Passing-based HGNNs	15
B.1	Expressiveness of CoNHD	15
B.2	Addressing the Limitations of Message Passing	15
C	Discussion on Other Hypergraph Neural Networks	16
D	Derivations and Proofs	17
D.1	Derivation of Eq. 7-9	17
D.2	Proof of Proposition 1	18
D.3	Proof of Proposition 2	18
D.4	Proof of Proposition 3	19
D.5	Proof of Proposition 4	19
E	Algorithms of CoNHD	20
F	Efficiency of CoNHD	21
F.1	Complexity Analysis	21
F.2	Efficiency Advantages in Mini-batch Training	22
G	Additional Details of the Datasets	22
H	Implementation Details	23
I	Supplementary Experimental Results	24
I.1	More Visualization of the Learned Embeddings	24

A Broader Impacts and Limitations

Broader Impacts. This paper proposes a novel and effective hypergraph neural network architecture based on hypergraph diffusion, which can effectively address the edge-dependent node classification problem. As shown in previous research [12], this problem is important and useful for a wide range of real-world applications, including product-return prediction [13], anomaly detection [16], ranking [14], and clustering [15]. The proposed method CoNHD demonstrates theoretical advantages compared to existing message passing-based solutions, and achieves significant improvements on real-world ENC datasets in our experiments. We believe this work can make contributions to these practical applications and bring positive social impacts.

This work is foundational research on hypergraph learning methods and is not tied to particular practical applications. Due to the improved expressiveness, one potential negative impact of this work is overfitting to biases present in the training data. To mitigate this risk, we recommend combining explainable graph techniques [74, 75] with the CoNHD method, which can help identify the sources of bias in the model and improve the fairness of the model decisions.

Limitations & Future Work. One limitation lies in the ISAB operator, which, unlike the UNP operator, lacks the universal property for approximating any set-equivariant functions, despite its superior performance in our experiments. Future investigations could explore more different universal set-equivariant neural networks [68] in the proposed CoNHD method. Another limitation is that

CoNHD only leverages initial features without incorporating the observed labels in the diffusion process. The observed edge-dependent labels of a node can help predict its unobserved edge-dependent labels. For example, an author frequently appears as the last author in many papers is more likely to be the last author in other papers as well. It is good to consider the label dependencies and extend this method for structured classification [76].

B Comparison to Message Passing-based HGNNs

In this section, we theoretically compare the proposed CoNHD model to message passing-based HGNNs, which can cover most existing hypergraph neural networks [18, 40]. We first show that CoNHD is expressive enough to represent any HGNNs following the message passing framework defined in Eq. 1-3. Subsequently, we discuss how CoNHD effectively addresses the three limitations of message passing as discussed in the introduction. We provide more discussion about some other HGNN models that do not follow the message passing framework in Appendix C.

B.1 Expressiveness of CoNHD

To demonstrate the expressiveness of CoNHD, we compare it with the message passing framework defined in Eq. 1-3, which can cover most existing hypergraph neural networks [18, 40].

To include more HGNN models in our comparison, we first show that some advanced methods, apart from many traditional message passing-based HGNNs discussed in [18, 40], can also be represented by the message passing framework. It is argued that the traditional message passing framework overlooks the importance of edge-dependent node information and passes the same node representation to different hyperedges [19]. Some advanced methods attempt to extract edge-dependent node representations before aggregation [20, 12]. Proposition 3 shows that these advanced methods with edge-dependent node information are also special cases of the message passing framework defined in Eq. 1-3.

Proposition 3. *ED-HNN [20], ED-HNNII [20], and WHATsNet [12] are special cases of the message passing framework defined in Eq. 1-3.*

The message passing framework can only generate separate representations for nodes and hyperedges. Following [12], we regard the concatenation of node and hyperedge representations as the co-representation, i.e., $\mathbf{h}_{v,e}^{(t)} = [\mathbf{x}_v^{(t)}, \mathbf{z}_e^{(t)}]$, which can be used to predict edge-dependent node labels.

Proposition 4. *With the same co-representation dimension, CoNHD is expressive enough to represent the message passing framework, while the opposite is not true.*

Proposition 4 demonstrates that CoNHD is more expressive than all methods following the message passing framework. Specifically, CoNHD models within-edge and within-node interactions as multi-input multi-output functions through two equivariant diffusion operators, which are more expressive than the invariant aggregation operators in the message passing framework.

Notably, despite the increased expressiveness, CoNHD still maintains a similar theoretical complexity compared to other HGNNs within the message passing framework such as WHATsNet [12]. We leave the detailed analysis to Appendix F.1.

B.2 Addressing the Limitations of Message Passing

Message passing models both within-edge and within-node interactions as multi-input single-output functions, which brings three limitations as discussed in the introduction. We show that CoNHD can effectively address these three limitations.

- **Non-adaptive representation size.**

In *message passing*, messages from numerous hyperedges/nodes are aggregated to a fixed-size node/edge representation vector. As indicated in [19], this can cause potential information loss for large-degree nodes or hyperedges. A possible solution is to assign a high-dimensional representation for each node or hyperedge. However, the high-dimensional representations increase the computational costs and can lead to training difficulty.

In *CoNHD*, the co-representations are related to node-hyperedge pairs. For larger-degree nodes or hyperedges, they are contained by more node-hyperedge pairs and therefore are associated with more co-representations. The number of co-representations adaptively scales with node or hyperedge degrees, which can prevent potential information loss.

- **Node/Edge agnostic messages.**

In *message passing*, since the aggregated node representation loses edge-dependent information, the node can only pass the same message to different hyperedges. However, different hyperedges may focus on different properties of the node and should receive different messages. While some methods attempt to extract edge-dependent information from one node representation [19, 20, 12], this extraction process increases the learning difficulty.

In *CoNHD*, the co-representations inherently preserve specific information for each node-hyperedge pair, which can serve as the edge-dependent node representation or node-dependent edge representation. Without the aggregation process, *CoNHD* avoids mixing different information into a single node or edge representations, and thus obviates the necessity of extracting edge-/node-dependent information, which can reduce the learning difficulty compared to those edge-dependent message passing methods.

- **Insufficient interactions among nodes or hyperedges.**

In *message passing*, the single-output design cannot include direct nodes-to-nodes or edges-to-edges interactions, as this requires multiple outputs for different elements. These interactions are shown to be critical for hypergraph learning [21].

In *CoNHD*, the co-representations include both node and hyperedge information. The interactions among co-representations naturally include not only interactions between nodes and hyperedges, but also direct nodes-to-nodes and edges-to-edges interactions.

Two critical designs of *CoNHD* are: (1) introducing the concept of co-representations, and (2) modeling interactions using equivariant diffusion operators. These two designs enable the modeling of both within-edge and within-node interactions as multi-input multi-output functions, which are more expressive than the single-output aggregation functions and can effectively address the three limitations in message passing.

C Discussion on Other Hypergraph Neural Networks

LEGCN [77] and MultiSetMixer [41] are two approaches that do not follow the message passing framework defined in Eq. 1-3 and can explicitly generate edge-dependent node representations, which are similar to the concept of co-representations in the proposed *CoNHD* model. Unfortunately, LEGCN transforms the hypergraph structure into a traditional graph structure, which loses some higher-order group information. Instead, MultiSetMixer preserves the hypergraph structure but still models it as a two-stage message passing process, where messages from nodes are aggregated to a single hyperedge representation and then back to nodes. Both of these two methods model within-edge and within-node interactions as multi-input single-output functions, which can only generate the same output for different node-hyperedge pairs and therefore limits their expressiveness.

LEGCN. LEGCN converts a hypergraph into a traditional graph using line expansion, and utilizes graph convolution [28] to learn representations of the new nodes on the expanded graph. The $(t+1)$ -th layer of LEGCN (without normalization) can be formulated as:

$$\begin{aligned} \mathbf{m}_e^{(t+1)} &= \sum_{v_i \in e} \mathbf{h}_{v_i, e}^{(t)}, \quad \mathbf{m}'_v{}^{(t+1)} = \sum_{e_j \in \mathcal{E}_v} \mathbf{h}_{v, e_j}^{(t)}, \\ \mathbf{h}_{v, e}^{(t+1)} &= \sigma(\lambda \mathbf{m}_e^{(t+1)} + \gamma \mathbf{m}'_v{}^{(t+1)}) \mathbf{W}^{(t)}, \end{aligned}$$

where $\sigma(\cdot)$ denotes the non-linear activation function. $\mathbf{m}_e^{(t)}$ and $\mathbf{m}'_v{}^{(t)}$ are the within-edge information and the within-node information, respectively.

Compared to *CoNHD*, LEGCN exhibits three main limitations. (1) *Lack of differentiation between within-edge and within-node interactions.* In a line expansion graph, the new vertices (node-hyperedge pairs) associated with the same hyperedge or the same node are connected by homogeneous edges, which overlooks the difference between these two kinds of relations. Although LEGCN utilizes different scalar weights to balance within-edge or within-node messages, this is still not expressive

enough compared to two different neural diffusion operators in CoNHD. (2) *Node/Edge agnostic messages*. LEGCN still follows the single-output setting which only generates one shared within-edge message $\mathbf{m}_e^{(t)}$ and one shared within-node message $\mathbf{m}_v^{(t)}$ using sum pooling, instead of diverse messages for different node-hyperedge pairs. (3) *High computational complexity*. The motivation for LEGCN is to reduce the hypergraph structure to a graph structure. This reduction loses the higher-order group information and requires additional computation for different node-hyperedge pairs. For example, the learning for representations of node-hyperedge pairs (v_1, e_1) and (v_1, e_2) are calculated separately, although they have the same within-node messages $\mathbf{m}_{v_1}^{(t+1)}$ which only needs to be computed once. In contrast, our proposed CoNHD method generates all diffusing information within the same node v_1 together using the node diffusion operator with linear complexity.

MultiSetMixer. MultiSetMixer replaces each node representation in the message passing framework with several edge-dependent node representations. However, it still follows the message passing framework and aggregates different node representations into a single edge representation. This models the within-edge interactions as multi-input single-output functions. The $(t+1)$ -th layer of MultiSetMixer can be formulated as:

$$\begin{aligned}\mathbf{m}_e^{(t+1)} &= \frac{1}{d_e} \sum_{v_i \in e} \mathbf{h}_{v_i, e}^{(t)} + \text{MLP}(\text{LN}(\frac{1}{d_e} \sum_{v_i \in e} \mathbf{h}_{v_i, e}^{(t)})), \\ \mathbf{h}_{v, e}^{(t+1)} &= \mathbf{h}_{v, e}^{(t)} + \text{MLP}(\text{LN}(\mathbf{h}_{v, e}^{(t)})) + \mathbf{m}_e^{(t+1)}.\end{aligned}$$

MultiSetMixer also generates one shared within-edge message $\mathbf{m}_e^{(t)}$, which loses specific messages for different node-hyperedge pair. This formulation still suffers from the three main limitations of the message passing framework. Besides, it does not incorporate within-node interactions, which cannot model the relationships among different representations associated with the same node.

D Derivations and Proofs

D.1 Derivation of Eq. 7-9

We use the ADMM method [63] to solve the optimization problem in Eq. 5 with non-differentiable functions. We first introduce an auxiliary variable $\mathbf{A}_e = \mathbf{H}_e$ for each hyperedge e , and an auxiliary variable $\mathbf{B}_v = \mathbf{H}_v$ for each node v . Then the problem in Eq. 5 can be

$$\begin{aligned}\min_{\mathcal{H}} \quad & \sum_{v \in \mathcal{V}} \sum_{e \in \mathcal{E}_v} \mathcal{R}_{v, e}(\mathbf{h}_{v, e}; \mathbf{a}_{v, e}) + \lambda \sum_{e \in \mathcal{E}} \Omega_e(\mathbf{A}_e) + \gamma \sum_{v \in \mathcal{V}} \Omega_v(\mathbf{B}_v), \\ \text{s.t.} \quad & \forall e \in \mathcal{E} : \mathbf{A}_e = \mathbf{H}_e, \\ & \forall v \in \mathcal{V} : \mathbf{B}_v = \mathbf{H}_v.\end{aligned}$$

Then the scaled form augmented Lagrangian function can be transformed as:

$$\begin{aligned}L_\rho &= \sum_{v \in \mathcal{V}} \sum_{e \in \mathcal{E}_v} \mathcal{R}_{v, e}(\mathbf{h}_{v, e}; \mathbf{a}_{v, e}) + \lambda \sum_{e \in \mathcal{E}} \Omega_e(\mathbf{A}_e) + \gamma \sum_{v \in \mathcal{V}} \Omega_v(\mathbf{B}_v) \\ &+ \sum_{e \in \mathcal{E}} \frac{\rho}{2} (\|\mathbf{A}_e - \mathbf{H}_e + \mathbf{P}_e\|_F^2 - \|\mathbf{P}_e\|_F^2) \\ &+ \sum_{v \in \mathcal{V}} \frac{\rho}{2} (\|\mathbf{B}_v - \mathbf{H}_v + \mathbf{Q}_v\|_F^2 - \|\mathbf{Q}_v\|_F^2),\end{aligned}$$

where \mathbf{P}_e and \mathbf{Q}_v are the scaled dual variables (with scaling factor $\frac{1}{\rho}$). Then we can use the primal-dual algorithms in ADMM to find the optimal solutions [63].

The primal steps can be calculated as follows:

$$\begin{aligned}\mathbf{A}_e^{(t+1)} &:= \arg \min_{\mathbf{A}_e} L_\rho \\ &= \arg \min_{\mathbf{A}_e} \frac{\lambda}{\rho} \Omega_e(\mathbf{A}_e) + \frac{1}{2} \|\mathbf{A}_e - \mathbf{H}_e^{(t)} + \mathbf{P}_e^{(t)}\|_F^2 \\ &= \text{prox}_{\lambda \Omega_e / \rho}(\mathbf{H}_e^{(t)} - \mathbf{P}_e^{(t)}), \forall e \in \mathcal{E},\end{aligned}$$

$$\begin{aligned}
\mathbf{B}_v^{(t+1)} &:= \arg \min_{\mathbf{B}_v} L_\rho \\
&= \arg \min_{\mathbf{B}_v} \frac{\gamma}{\rho} \Omega_v(\mathbf{B}_v) + \frac{1}{2} \|\mathbf{B}_v - \mathbf{H}_v^{(t)} + \mathbf{Q}_v^{(t)}\|_F^2 \\
&= \mathbf{prox}_{\gamma \Omega_v / \rho}(\mathbf{H}_v^{(t)} - \mathbf{Q}_v^{(t)}), \forall v \in \mathcal{V}, \\
\mathbf{h}_{v,e}^{(t+1)} &:= \arg \min_{\mathbf{h}_{v,e}} L_\rho \\
&= \arg \min_{\mathbf{h}_{v,e}} \mathcal{R}_{v,e}(\mathbf{h}_{v,e}; \mathbf{a}_{v,e}) + \frac{\rho}{2} \|\mathbf{h}_{v,e} - [\mathbf{A}_e^{(t+1)}]_v - [\mathbf{P}_e^{(t)}]_v\|_2^2 \\
&\quad + \frac{\rho}{2} \|\mathbf{h}_{v,e} - [\mathbf{B}_v^{(t+1)}]_e - [\mathbf{Q}_v^{(t)}]_e\|_2^2 \\
&= \arg \min_{\mathbf{h}_{v,e}} \frac{1}{2\rho} \mathcal{R}_{v,e}(\mathbf{h}_{v,e}; \mathbf{a}_{v,e}) \\
&\quad + \frac{1}{2} \left\| \mathbf{h}_{v,e} - \frac{1}{2} ([\mathbf{A}_e^{(t+1)}]_v + [\mathbf{P}_e^{(t)}]_v + [\mathbf{B}_v^{(t+1)}]_e + [\mathbf{Q}_v^{(t)}]_e) \right\|_2^2 \\
&= \mathbf{prox}_{\mathcal{R}_{v,e}(\cdot; \mathbf{a}_{v,e}) / 2\rho} \left(\frac{1}{2} ([\mathbf{A}_e^{(t+1)}]_v + [\mathbf{P}_e^{(t)}]_v + [\mathbf{B}_v^{(t+1)}]_e + [\mathbf{Q}_v^{(t)}]_e) \right), \forall e \in \mathcal{E}_v, \forall v \in \mathcal{V}.
\end{aligned}$$

The dual steps can be calculated as follows:

$$\begin{aligned}
\mathbf{P}_e^{(t+1)} &:= \mathbf{P}_e^{(t)} + \mathbf{A}_e^{(t+1)} - \mathbf{H}_e^{(t+1)}, \forall e \in \mathcal{E}, \\
\mathbf{Q}_v^{(t+1)} &:= \mathbf{Q}_v^{(t)} + \mathbf{B}_v^{(t+1)} - \mathbf{H}_v^{(t+1)}, \forall v \in \mathcal{V}.
\end{aligned}$$

By defining $\mathbf{U}_e^{(t+1)} = \mathbf{A}_e^{(t+1)} + \mathbf{P}_e^{(t)}$ and $\mathbf{Z}_v^{(t+1)} = \mathbf{B}_v^{(t+1)} + \mathbf{Q}_v^{(t)}$, the update process can be simplified as follows:

$$\begin{aligned}
\mathbf{U}_e^{(t+1)} &= \mathbf{prox}_{\lambda \Omega_e / \rho}(2\mathbf{H}_e^{(t)} - \mathbf{U}_e^{(t)}) + \mathbf{U}_e^{(t)} - \mathbf{H}_e^{(t)}, \forall e \in \mathcal{E}, \\
\mathbf{Z}_v^{(t+1)} &= \mathbf{prox}_{\gamma \Omega_v / \rho}(2\mathbf{H}_v^{(t)} - \mathbf{Z}_v^{(t)}) + \mathbf{Z}_v^{(t)} - \mathbf{H}_v^{(t)}, \forall v \in \mathcal{V}, \\
\mathbf{h}_{v,e}^{(t+1)} &= \mathbf{prox}_{\mathcal{R}_{v,e}(\cdot; \mathbf{a}_{v,e}) / 2\rho} \left(\frac{1}{2} ([\mathbf{U}_e^{(t+1)}]_v + [\mathbf{Z}_v^{(t+1)}]_e) \right), \forall e \in \mathcal{E}_v, \forall v \in \mathcal{V}.
\end{aligned}$$

D.2 Proof of Proposition 1

Proposition 1 (Wang et al. [20]). *With permutation invariant structural regularization functions, the diffusion operators are permutation equivariant.*

Proof. Proved in Proposition 2 in [20]. □

D.3 Proof of Proposition 2

Proposition 2. *The node-representation hypergraph diffusion is a special case of the co-representation hypergraph diffusion.*

Proof. We first rewrite the node-representation hypergraph diffusion defined in Eq. 4 as a constraint optimization problem, then show that it is a special case of co-representation hypergraph diffusion defined in Eq. 5.

For each $v \in \mathcal{V}$, we introduce a set of new variable $\{\mathbf{h}_{v,e_i} | e_i \in \mathcal{E}_v\}$, satisfying $\mathbf{h}_{v,e_1} = \mathbf{x}_v$, and $\mathbf{h}_{v,e_i} = \mathbf{h}_{v,e_j}$ for any $e_i, e_j \in \mathcal{E}_v$. Then the objective function in Eq. 4 becomes:

$$\begin{aligned}
\sum_{v \in \mathcal{V}} \mathcal{R}_v(\mathbf{x}_v; \mathbf{a}_v) + \lambda \sum_{e \in \mathcal{E}} \Omega_e(\mathbf{X}_e) &= \sum_{v \in \mathcal{V}} \sum_{e \in \mathcal{E}_v} \frac{1}{d_v} \mathcal{R}_v(\mathbf{x}_v; \mathbf{a}_v) + \lambda \sum_{e \in \mathcal{E}} \Omega_e(\mathbf{X}_e) \\
&= \sum_{v \in \mathcal{V}} \sum_{e \in \mathcal{E}_v} \frac{1}{d_v} \mathcal{R}_v(\mathbf{h}_{v,e}; \mathbf{a}_v) + \lambda \sum_{e \in \mathcal{E}} \Omega_e(\mathbf{H}_e),
\end{aligned}$$

The original problem in Eq. 4 can be reformulated as a constraint optimization problem:

$$\begin{aligned} \arg \min_{\mathbf{H}} \quad & \sum_{v \in \mathcal{V}} \sum_{e \in \mathcal{E}_v} \frac{1}{d_v} \mathcal{R}_v(\mathbf{h}_{v,e}; \mathbf{a}_v) + \lambda \sum_{e \in \mathcal{E}} \Omega_e(\mathbf{H}_e), \\ \text{s.t.} \quad & \forall v \in \mathcal{V}, \forall e_i, e_j \in \mathcal{E}_v : \mathbf{h}_{v,e_i} = \mathbf{h}_{v,e_j}, \end{aligned} \quad (\text{A1})$$

where the optimal solutions satisfy $\mathbf{h}_{v,e}^* = \mathbf{x}_v^*$.

We now show that this constraint optimization is a special case of co-representation hypergraph diffusion. We can set $\mathcal{R}_{v,e}(\cdot; \mathbf{a}_{v,e}) = \frac{1}{d_v} \mathcal{R}_v(\cdot; \mathbf{a}_v)$, and use the CE regularization functions [52] for the node regularization functions in Eq. 5, i.e., $\Omega_{\text{CE}}(\mathbf{H}_v) := \sum_{e_i, e_j \in \mathcal{E}_v} \|\mathbf{h}_{v,e_i} - \mathbf{h}_{v,e_j}\|_2^2$. Then Eq. 5 can be reformulated as follows:

$$\arg \min_{\mathbf{H}} \sum_{v \in \mathcal{V}} \sum_{e \in \mathcal{E}_v} \frac{1}{d_v} \mathcal{R}_v(\mathbf{h}_{v,e}; \mathbf{a}_v) + \lambda \sum_{e \in \mathcal{E}} \Omega_e(\mathbf{H}_e) + \gamma \sum_{v \in \mathcal{V}} \Omega_{\text{CE}}(\mathbf{H}_v). \quad (\text{A2})$$

The node regularization term in A2 is exactly the exterior penalty function [78] for the given equality constraints in Eq. A1. Thus when $\gamma \rightarrow \infty$, Eq. A2 yields the same optimal solutions as Eq. A1. \square

D.4 Proof of Proposition 3

Proposition 3. *ED-HNN [20], ED-HNNII [20], and WHATsNet [12] are special cases of the message passing framework defined in Eq. 1-3.*

Proof. For ED-HNN [20], each layer can be represented as:

$$\begin{aligned} \mathbf{z}_e^{(t+1)} &= f_{\mathcal{V} \rightarrow \mathcal{E}}(\mathbf{X}_e^{(t)}; \mathbf{z}_e^{(t)}) = \frac{1}{d_e} \sum_{u \in e} \text{MLP}(\mathbf{x}_u^{(t)}), \\ \tilde{\mathbf{x}}_v^{(t+1)} &= f_{\mathcal{E} \rightarrow \mathcal{V}}(\mathbf{Z}_v^{(t+1)}; \mathbf{x}_v^{(t)}) = \frac{1}{d_v} \sum_{e: v \in e} \text{MLP}([\mathbf{z}_e^{(t+1)}, \mathbf{x}_v^{(t)}]), \\ \mathbf{x}_v^{(t+1)} &= f_{\text{skip}}(\tilde{\mathbf{x}}_v^{(t+1)}, \mathbf{x}_v^{(t)}, \mathbf{x}_v^{(0)}) = \text{MLP}(\tilde{\mathbf{x}}_v^{(t+1)}, \mathbf{x}_v^{(t)}, \mathbf{x}_v^{(0)}), \end{aligned}$$

where $[\dots]$ denotes concatenation in the last dimension. The degree of hyperedge e and node v , denoted as d_e and d_v , can be obtained from the number of rows in $\mathbf{X}_e^{(t)}$ and $\mathbf{Z}_v^{(t+1)}$. ED-HNN ignores the hyperedge representation $\mathbf{z}_e^{(t)}$ in the first aggregation function $f_{\mathcal{V} \rightarrow \mathcal{E}}$.

For ED-HNNII, the only difference compared to ED-HNN is the function $f_{\mathcal{V} \rightarrow \mathcal{E}}$, which concatenates the edge and node features to generate node-dependent edge representation. The function $f_{\mathcal{V} \rightarrow \mathcal{E}}$ can be represented as:

$$\mathbf{z}_e^{(t+1)} = f_{\mathcal{V} \rightarrow \mathcal{E}}(\mathbf{X}_e^{(t)}; \mathbf{z}_e^{(t)}) = \frac{1}{d_e} \sum_{u \in e} \text{MLP}([\mathbf{x}_u^{(t)}, \mathbf{z}_e^{(t)}]).$$

For WHATsNet, we ignore the positional encoding part which can be combined with the input, and focus on the HGNN architecture. Each layer of WHATsNet can then be represented as:

$$\begin{aligned} \mathbf{z}_e^{(t+1)} &= f_{\mathcal{V} \rightarrow \mathcal{E}}(\mathbf{X}_e^{(t)}; \mathbf{z}_e^{(t)}) = \text{MAB}(\mathbf{z}_e^{(t)\top}, \text{ISAB}(\mathbf{X}_e^{(t)}))^\top, \\ \tilde{\mathbf{x}}_v^{(t+1)} &= f_{\mathcal{E} \rightarrow \mathcal{V}}(\mathbf{Z}_v^{(t+1)}; \mathbf{x}_v^{(t)}) = \text{MAB}(\mathbf{x}_v^{(t)\top}, \text{ISAB}(\mathbf{Z}_v^{(t+1)}))^\top, \\ \mathbf{x}_v^{(t+1)} &= f_{\text{skip}}(\tilde{\mathbf{x}}_v^{(t+1)}, \mathbf{x}_v^{(t)}, \mathbf{x}_v^{(0)}) = \tilde{\mathbf{x}}_v^{(t+1)}, \end{aligned}$$

where $\text{MAB}(\cdot)$ and $\text{ISAB}(\cdot)$ denote the multihead attention block and the induced set attention block in Set Transformer [69], as described in the main paper. WHATsNet does not include skip connections and therefore ignores the original node feature $\mathbf{x}_v^{(0)}$ in f_{skip} . \square

D.5 Proof of Proposition 4

Proposition 4. *With the same co-representation dimension, CoNHD is expressive enough to represent the message passing framework, while the opposite is not true.*

Proof. We prove the proposition using the GD-based implementation of CoNHD, which can be easily extended to the ADMM-based implementation.

First, we prove that CoNHD is expressive enough to represent any model within the message passing framework. We initialize the co-representations as $\mathbf{h}_{v,e}^{(0)} = [\mathbf{x}_v^{(0)}, \mathbf{z}_e^{(0)}]$. For brevity, we assume $\mathbf{x}_v^{(0)} \in \mathbb{R}^{\frac{d}{2}}$ and $\mathbf{z}_e^{(0)} \in \mathbb{R}^{\frac{d}{2}}$. We will show that given $\mathbf{h}_{v,e}^{(2t)} = [\mathbf{x}_v^{(t)}, \mathbf{z}_e^{(t)}]$, two layers of CoNHD are expressive enough to generate $\mathbf{h}_{v,e}^{(2(t+1))} = [\mathbf{x}_v^{(t+1)}, \mathbf{z}_e^{(t+1)}]$, where $\mathbf{x}_v^{(t)}$ and $\mathbf{z}_e^{(t)}$ are exactly correspond to the node and hyperedge representations in the t -th layer of the message passing framework defined in Eq. 1-3.

When ϕ and φ are implemented by universal equivariant neural diffusion operators like UNP, they are expressive enough to represent any equivariant mapping. With the same co-representation dimension, we can use one layer in CoNHD to represent the nodes-to-edge aggregation process in the message passing framework. In this layer, we reduce ϕ , φ , and ψ as follows:

$$\begin{aligned} \mathbf{M}_e^{(2t+1)} &= \phi(\mathbf{H}_e^{(2t)}) = [\mathbf{0}_{d_e \times \frac{d}{2}}, \mathbf{1}_{d_e} \cdot (f_{\mathcal{V} \rightarrow \mathcal{E}}(\mathbf{X}_e^{(t)}; \mathbf{z}_e^{(t)}))^\top] \\ &= [\mathbf{0}_{d_e \times \frac{d}{2}}, \mathbf{1}_{d_e} \cdot \mathbf{z}_e^{(t+1)\top}], \\ \mathbf{M}_v'^{(2t+1)} &= \varphi(\mathbf{H}_v^{(2t)}) = [\mathbf{0}_{d_v \times \frac{d}{2}}, \mathbf{0}_{d_v \times \frac{d}{2}}], \\ \mathbf{h}_{v,e}^{(2t+1)} &= \psi([\mathbf{h}_{v,e}^{(2t)}, \mathbf{m}_{v,e}^{(2t+1)}, \mathbf{m}_{v,e}'^{(2t+1)}, \mathbf{h}_{v,e}^{(0)}]) = [\mathbf{x}_v^{(t)}, \mathbf{z}_e^{(t+1)}], \end{aligned}$$

where $\mathbf{1}_n$ represents a n -dimensional all one vector, which is used to construct a matrix with repeated row elements. $\mathbf{0}_{m \times n}$ represents a $(m \times n)$ -dimensional all zero matrix. In this layer, we use ϕ to represent the aggregation process and ignore the output of φ .

We use another layer to represent the edges-to-node aggregation process and the skip connection. In this layer, we reduce ϕ , φ , and ψ as follows:

$$\begin{aligned} \mathbf{M}_e^{(2(t+1))} &= \phi(\mathbf{H}_e^{(2t+1)}) = [\mathbf{0}_{d_e \times \frac{d}{2}}, \mathbf{0}_{d_e \times \frac{d}{2}}], \\ \mathbf{M}_v'^{(2(t+1))} &= \varphi(\mathbf{H}_v^{(2t+1)}) = [\mathbf{1}_{d_v} \cdot (f_{\mathcal{E} \rightarrow \mathcal{V}}(\mathbf{Z}_v^{(t+1)}; \mathbf{x}_v^{(t)}))^\top, \mathbf{0}_{d_e \times \frac{d}{2}}] \\ &= [\mathbf{1}_{d_v} \cdot \tilde{\mathbf{x}}_v^{(t+1)\top}, \mathbf{0}_{d_e \times \frac{d}{2}}], \\ \mathbf{h}_{v,e}^{(2(t+1))} &= \psi([\mathbf{h}_{v,e}^{(2t+1)}, \mathbf{m}_{v,e}^{(2(t+1))}, \mathbf{m}_{v,e}'^{(2(t+1))}, \mathbf{h}_{v,e}^{(0)}]) \\ &= [f_{\text{skip}}(\mathbf{x}_v^{(t)}, \tilde{\mathbf{x}}_v^{(t+1)}, \mathbf{x}_v^{(0)}), \mathbf{z}_e^{(t+1)}] \\ &= [\mathbf{x}_v^{(t+1)}, \mathbf{z}_e^{(t+1)}]. \end{aligned}$$

In this layer, we use φ to represent the aggregation process and ignore the output of ϕ . Besides, we set the update function ψ to represent the skip connection part. The final output $\mathbf{x}_v^{(t+1)}$ and $\mathbf{z}_e^{(t+1)}$ are the $(t+1)$ -th node and hyperedge representation in the message passing framework. Therefore, CoNHD is expressive enough to represent any model within the message passing framework.

To show that the opposite is not true, we only need to construct a counter-example. Since ϕ is equivariant, it can generate different diffusing information $\mathbf{m}_{v,e}^{(t)}$ for different node-hyperedge pair (v, e) . We can simply set $\mathbf{h}_{v,e}^{(t)} = \mathbf{m}_{v,e}^{(t)}$ in the update function ψ , which lead to different representation for each node-hyperedge pair (v, e) . However, the message passing framework can only generate the same hyperedge representation for each hyperedge, which constraints that the first $\frac{d}{2}$ dimension of the co-representations for different node-hyperedge pairs are the same and cannot generate the same $\mathbf{h}_{v,e}^{(t)}$. Therefore, any model within the message passing framework cannot represent CoNHD. \square

E Algorithms of CoNHD

Algorithm 1 and 2 describe the forward propagation of the CoNHD model for edge-dependent node classification using GD-based and ADMM-based implementations, respectively. ϕ and φ are implemented as UNP (Eq. 10) or ISAB (Eq. 11). Although the proposed CoNHD model can accept any features related to the node-hyperedge pairs, we initialize the co-representations using only the node features to follow the setup of the original ENC problem [12].

Algorithm 1: CoNHD-GD for edge-dependent node classification.

Input : A hypergraph $\mathcal{G} = (\mathcal{V}, \mathcal{E})$, an initial node feature matrix $\mathbf{X}^{(0)} = [\mathbf{x}_{v_1}^{(0)}, \dots, \mathbf{x}_{v_n}^{(0)}]^\top$.

Output : Predicted edge-dependent node labels $\hat{y}_{v,e}$.

Initialize $\forall v \in \mathcal{V}, \forall e \in \mathcal{E}_v : \mathbf{h}_{v,e}^{(0)} = \mathbf{x}_v^{(0)}$;

for $\ell = 1, \dots, L$ **do**

// within-edge interactions (Eq. 12).

$\forall e \in \mathcal{E} : \mathbf{M}_e^{(\ell)} \leftarrow \phi(\mathbf{H}_e^{(\ell-1)})$;

// within-node interactions (Eq. 12).

$\forall v \in \mathcal{V} : \mathbf{M}_v'^{(\ell)} \leftarrow \varphi(\mathbf{H}_v^{(\ell-1)})$;

// co-representation updates (Eq. 13).

$\forall v \in \mathcal{V}, \forall e \in \mathcal{E}_v : \mathbf{h}_{v,e}^{(\ell)} \leftarrow \psi([\mathbf{h}_{v,e}^{(\ell-1)}, \mathbf{m}_{v,e}^{(\ell)}, \mathbf{m}_{v,e}'^{(\ell)}, \mathbf{h}_{v,e}^{(0)}])$;

end

for $v \in \mathcal{V}, e \in \mathcal{E}_v$ **do**

 Predict edge-dependent node label $\hat{y}_{v,e}$ using co-representation $\mathbf{h}_{v,e}^{(L)}$.

end

Algorithm 2: CoNHD-ADMM for edge-dependent node classification.

Input : A hypergraph $\mathcal{G} = (\mathcal{V}, \mathcal{E})$, an initial node feature matrix $\mathbf{X}^{(0)} = [\mathbf{x}_{v_1}^{(0)}, \dots, \mathbf{x}_{v_n}^{(0)}]^\top$.

Output : Predicted edge-dependent node labels $\hat{y}_{v,e}$.

Initialize $\forall v \in \mathcal{V}, \forall e \in \mathcal{E}_v : \mathbf{h}_{v,e}^{(0)} = \mathbf{x}_v^{(0)}, \mathbf{m}_{v,e}^{(0)} = \mathbf{h}_{v,e}^{(0)}, \mathbf{m}_{v,e}'^{(0)} = \mathbf{h}_{v,e}^{(0)}$;

for $\ell = 1, \dots, L$ **do**

// within-edge interactions (Eq. 14).

$\forall e \in \mathcal{E} : \mathbf{M}_e^{(\ell)} \leftarrow \phi(2\mathbf{H}_e^{(\ell-1)} - \mathbf{M}_e^{(\ell-1)}) + \mathbf{M}_e^{(\ell-1)} - \mathbf{H}_e^{(\ell-1)}$;

// within-node interactions (Eq. 15).

$\forall v \in \mathcal{V} : \mathbf{M}_v'^{(\ell)} \leftarrow \varphi(2\mathbf{H}_v^{(\ell-1)} - \mathbf{M}_v'^{(\ell-1)}) + \mathbf{M}_v'^{(\ell-1)} - \mathbf{H}_v^{(\ell-1)}$;

// co-representation updates (Eq. 16).

$\forall v \in \mathcal{V}, \forall e \in \mathcal{E}_v : \mathbf{h}_{v,e}^{(\ell)} \leftarrow \psi([\mathbf{m}_{v,e}^{(\ell)}, \mathbf{m}_{v,e}'^{(\ell)}, \mathbf{h}_{v,e}^{(0)}])$;

end

for $v \in \mathcal{V}, e \in \mathcal{E}_v$ **do**

 Predict edge-dependent node label $\hat{y}_{v,e}$ using co-representation $\mathbf{h}_{v,e}^{(L)}$.

end

F Efficiency of CoNHD

F.1 Complexity Analysis

We discuss the complexity of two GD-based implementations using UNP or ISAB operators, while the ADMM-based implementations have similar results.

Both the UNP and ISAB operators have linear complexity with the number of the input co-representations. For the UNP implementation, the first MLP and the sum pooling only calculate once for all elements in the set, and the second MLP calculates in an element-wise manner. We set the same hidden size as the co-representation size for MLPs. With co-representation dimension d , the overall complexity for the within-edge and within-node interactions in each layer is $\mathcal{O}(\sum_{e \in \mathcal{E}} (d_e d^2) + \sum_{v \in \mathcal{V}} (d_v d^2)) = \mathcal{O}(d^2 \sum_{e \in \mathcal{E}} d_e)$. This equation follows from the fact that the sum of node degrees is equal to the sum of hyperedge degrees, i.e., $\sum_{v \in \mathcal{V}} d_v = \sum_{e \in \mathcal{E}} d_e$. The ISAB implementation requires dot products between the input co-representations and k inducing points. The overall complexity for the within-edge and within-node interactions in each layer is $\mathcal{O}(\sum_{e \in \mathcal{E}} (d_e k d + (d_e + k) d^2) + \sum_{v \in \mathcal{V}} (d_v k d + (d_v + k) d^2)) = \mathcal{O}((dk + d^2) \sum_{e \in \mathcal{E}} d_e + \sum_{e \in \mathcal{E}} k d^2 + \sum_{v \in \mathcal{V}} k d^2)$. When k is small (in our experiments, $k = 4$), this complexity can be simplified as $\mathcal{O}(d^2 \sum_{e \in \mathcal{E}} d_e)$, which is consistent with the UNP implementation. For the update function, the

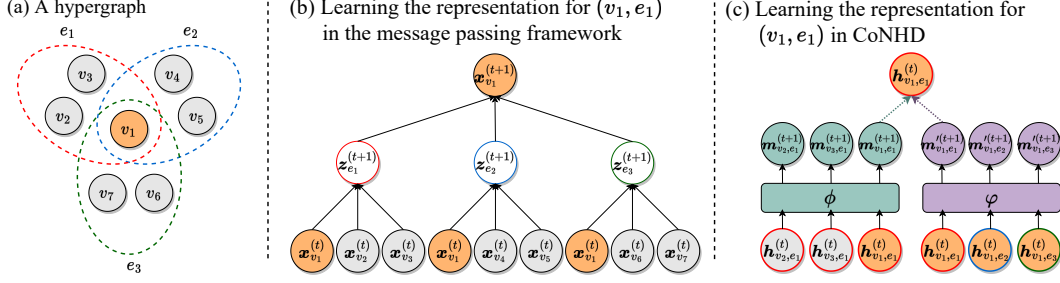


Figure A1: **Learning the representation for a node-hyperedge pair in mini-batch training.** (a) An example hypergraph, where node v_1 and all hyperedges have degree 3. We want to learn the representation for node-hyperedge pair (v_1, e_1) . (b) In the message passing framework, each layer performs a two-stage aggregation process: from nodes to hyperedges and from hyperedges back to nodes. This process involves all nodes in the neighboring hyperedges of node v_1 . Some nodes (e.g., v_4, v_5, v_6 , and v_7) are not direct neighbors for the node-hyperedge pair (v_1, e_1) . (c) In contrast, CoNHD focuses solely on the direct neighbors in each layer, including neighboring edges of v_1 (i.e., e_1, e_2 , and e_3) and neighboring nodes of e_1 (i.e., v_1, v_2 , and v_3). This not only ensures the diffusing information is from the most related neighbors, but also reduces the subgraph size in each layer and improves the efficiency.

complexity is $\mathcal{O}(d^2 \sum_{e \in \mathcal{E}} d_e)$. Therefore, the overall complexity of CoNHD is $\mathcal{O}(Ld^2 \sum_{e \in \mathcal{E}} d_e)$, where L is the number of layers.

The overall complexity is linear to the number of node-hyperedge pairs in the input hypergraph, i.e., $\sum_{e \in \mathcal{E}} d_e$. This is similar to many HGNNs within the message passing framework, e.g., the best baseline method WHATsNet [12] in the ENC experiments.

F.2 Efficiency Advantages in Mini-batch Training

Despite the same theoretical computational complexity, CoNHD exhibits additional efficiency advantages in mini-batch training as shown in Section 5.1. Compared to full-batch training, mini-batch training is a more common setting for training on large real-world hypergraphs, which can reduce memory consumption. In mini-batch training, the overlapping of the subgraphs across different batches introduces additional computational overhead compared to full-batch training. The computational load scales with the size of the neighboring subgraph, i.e., the number of neighboring hyperedges and nodes.

For convenience, we assume all the node degrees and hyperedge degrees are equal to d_n . To calculate the representation for each node-hyperedge pair, in each layer, the message passing framework needs to calculate the two-stage aggregation process $\mathcal{V} \rightarrow \mathcal{E}$ and $\mathcal{E} \rightarrow \mathcal{V}$. This leads to a neighboring subgraph containing d_n hyperedges and d_n^2 nodes. As shown in Fig. A1(b), this process not only increases the computational complexity but also includes nodes that are not direct neighbors for the target node-hyperedge pair, which may affect the learning results. In contrast, each layer of CoNHD only contains direct neighboring hyperedges and nodes, as shown in Fig. A1(c), resulting in a smaller subgraph with d_n hyperedges and d_n nodes. This can greatly improve the efficiency when handling complex hypergraphs with large node and hyperedge degrees.

G Additional Details of the Datasets

Table A1 provides a comprehensive overview of the datasets used in our experiments.

We use all six real-world edge-dependent node classification datasets utilized in [12]. These datasets are Email (Email-Enron¹ and Email-Eu [79]), StackOverflow (Stack-Biology² and Stack-Physics²), and Co-authorship networks (Coauth-DBLP [80] and Coauth-AMiner³). In

¹<https://www.cs.cmu.edu/~enron/>

²<https://archive.org/download/stackexchange>

³<https://www.aminer.org/aminer-network>

Table A1: Detailed statistics of the datasets.

Dataset	Num. of Nodes	Num. of Edges	Avg. d_v	Avg. d_e	Med. d_v	Med. d_e	Max. d_v	Max. d_e	Min. d_v	Min. d_e
Email-Enron	21,251	101,124	55.83	11.73	8	6	18,168	948	1	3
Email-Eu	986	209,508	549.54	2.59	233	2	8,659	59	1	2
Stack-Biology	15,490	26,823	3.63	2.10	1	2	1,318	12	1	1
Stack-Physics	80,936	200,811	5.93	2.39	1	2	6,332	48	1	1
Coauth-DBLP	108,484	91,266	2.96	3.52	1	3	236	36	1	2
Coauth-AMiner	1,712,433	2,037,605	3.03	2.55	1	2	752	115	1	1
Senate	282	315	19.18	17.17	15	19	63	31	1	4

Email-Enron and Email-Eu, nodes represent individuals, and emails act as hyperedges connecting them. The edge-dependent node labels denote the role of a user within an email (sender, receiver, or CC’ed). In Stack-Biology and Stack-Physics, nodes represent users while posts on Stack Overflow are hyperedges. The edge-dependent node label indicates the role of a user within a post (questioner, chosen answerer, or other answerer). In Coauth-DBLP and Coauth-AMiner, publications serve as hyperedges connecting authors (nodes) in these datasets. The edge-dependent node label represents the order of an author within a publication (first, last, or others).

For the diffusion operator approximation experiment, we generate semi-synthetic diffusion data using the Senate [73] dataset with the same initial features $\mathcal{X}^{(0)}$ as the experiments in [20]. In Senate, nodes represent individual US Senators, while each hyperedge connects the sponsor and co-sponsors of a bill introduced in the Senate. Although our proposed CoNHD model can accept any input features related to the node-hyperedge pairs, we only utilize initial node features to fit the input of most HGNNs. Following [20], we sample one-dimensional node feature by the Gaussian distribution $\mathcal{N}(\mu, \sigma)$, where $\mu = 0$ and σ uniformly sampled from $[1, 10]$. We initialize the features of node-hyperedges using the node features, *i.e.*, $\mathcal{H}^{(0)} = \{\mathbf{x}_v^{(0)} | v \in \mathcal{V}, e \in \mathcal{E}_v\}$. We then generate the labels $\mathcal{H}^{(2)}$ by performing two steps of the co-representation hypergraph diffusion process. We consider three different diffusion operators: CE [52], TV ($p = 2$) [53], and LEC ($p = 2$) [54]. We apply gradient descent for the differential diffusion operator CE, and ADMM for the non-differential diffusion operators TV and LEC. We set equal weights for the node and edge regularization functions, *i.e.*, $\lambda = \gamma = 1$. We choose α and ρ to make the variance ratio $\text{Var}(\mathcal{H}^{(2)})/\text{Var}(\mathcal{H}^{(0)})$ in a similar scale. Specifically, we set the step size $\alpha = 0.06$ for CE in gradient descent, and set the scale factor $\rho = 0.07$ for TV and $\rho = 0.5$ for LEC in the ADMM optimization process. To avoid the node features exposed in the training process, we generate 100 pairs $(\mathcal{H}^{(0)}, \mathcal{H}^{(2)})$ using the same hypergraph structure, where 20 pairs are for the valid set and 20 pairs are for the test set.

H Implementation Details

To ensure a fair comparison, we follow the experimental setup for edge-dependent node classification in [12]. All models are tuned using grid search. Specifically, the learning rate is chosen from $\{0.0001, 0.001\}$ and the number of layers is chosen from $\{1, 2\}$. The batch size is set from $\{256, 512\}$ for the Coauth-AMiner dataset due to the large node number, while for other datasets the batch size is chosen from $\{64, 128\}$. To maintain consistent computational cost across methods, we fix the embedding dimension for node and hyperedge representations in baseline methods, and co-representations in the proposed CoNHD method, to 128. The dropout rate is set to 0.7. We run the models for 100 epochs with early stopping. For the implementation of the ISAB operator, we set the number of inducing points to 4 as WHATsNet, and use 2 attention layers. During training, we sample 40 neighboring hyperedges of a node, while we do not sample neighboring nodes of a hyperedge since the final label is related to all nodes in a hyperedge. HCHA [36] and HNN [19] are run in full-batch training with more epochs as in [12]. As different diffusion steps utilize the same diffusion operators in hypergraph diffusion, we share the weights in different layers of the proposed CoNHD model. We employ the same relative positional encoding as in the experiments of WHATsNet [12], which has shown effectiveness in predicting edge-dependent node labels.

For the diffusion operator approximation experiment, most hyperparameters follow the same setting as the ENC experiment. To ensure the expressive power of all models, we use a relatively large embedding dimension 256. The number of layers is fixed to 2, which is consistent with the steps of the diffusion process for generating the labels.

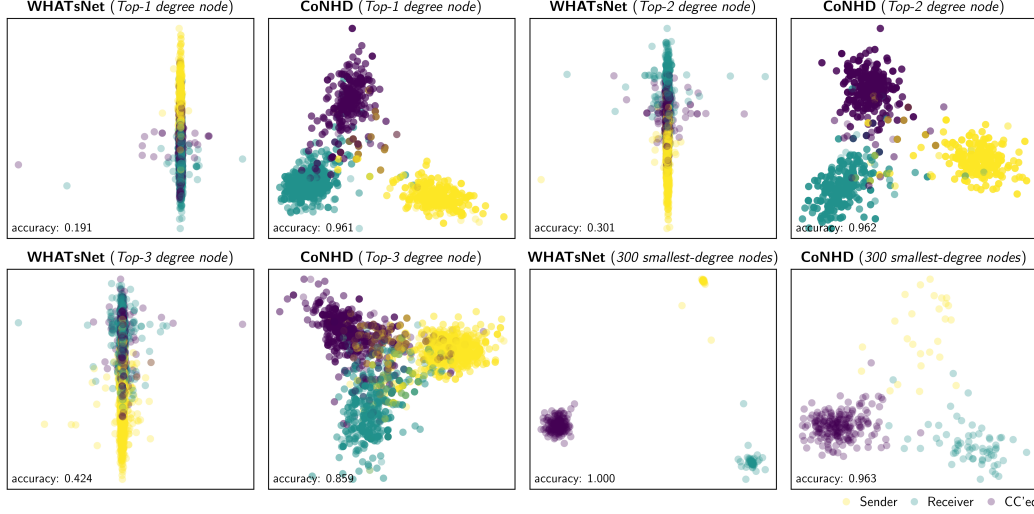


Figure A2: **More Visualization of embeddings in the Email-Enron dataset using LDA.** WHATsNet fails to learn separable embedding for node-hyperedge pairs associated with large-degree nodes, while the embeddings learned by CoNHD exhibit clearer distinctions. For small-degree nodes, both methods can learn separable embeddings for node-hyperedge pairs.

We conduct all experiments on a single NVIDIA A100 GPU with 40GB of GPU memory. To ensure statistically significant results, we repeat each experiment with 5 different random seeds and report the mean performance along with the standard deviation.

I Supplementary Experimental Results

I.1 More Visualization of the Learned Embeddings

We visualize the learned embeddings of node-hyperedge pairs in the Email-Enron dataset using LDA. As the same node can have different labels in different hyperedges, we choose the three largest-degree nodes and present the node-hyperedge embeddings associated with each of them. For the small-degree nodes, as these nodes are incident in fewer hyperedges, we visualize the node-hyperedge embeddings of the total 300 smallest-degree nodes. As shown in Fig. A2, CoNHD can learn more separable embeddings compared to the best baseline method WHATsNet on large-degree nodes. For the small-degree nodes, the embeddings from both methods can show clear distinction based on the edge-dependent node labels. CoNHD implements the interactions as multi-input multi-output functions, which can preserve specific information for each node-hyperedge pair and avoid potential information loss. This leads to significant performance improvements on the ENC task, especially for complex hypergraphs with large-degree nodes and hyperedges.